OPTICAL CAUSTICS FROM LIQUID DROPS UNDER GRAVITY: OBSERVATIONS OF THE PARABOLIC AND SYMBOLIC UMBILICS

By J. F. NYE, F.R.S.
H. H. Wills Physics Laboratory, University of Bristol, Tyndall Avenue, Bristol BS8 1TL, U.K.

(*Received* 31 *July* 1978)

[Plates 1–8]

CONTENTS

An earlier paper (Nye 1978) discussed the caustics formed by refraction of light in a thin gravity-free water drop resting on a glass surface. Here the effect of gravity is examined. In an irregular drop clinging to an inclined glass surface all the elementary catastrophes of co-dimension up to three are seen, including the hyperbolic umbilic. By suitably controlling the shape of the drop one can produce the higher-order singularities D_5 (parabolic umbilic) and E_6 (symbolic umbilic) with their corresponding unfoldings. The local topology of E_6 is accompanied by characteristic global topology signifying the presence of a higher organizing centre. Recognizing the typical unfolding patterns of D_5 and E_6 makes it possible to understand part of the complex pattern of interaction of the caustics from a thin irregular drop under gravity.

D_5 and E_6 are to be expected theoretically when a wave is refracted by a surface which is shaped by the combined effects of surface tension and gravity. The calculated relation

between the canonical control parameters of these catastrophes and the physical controls, such as focusing, gives a satisfactory explanation of what is seen. Three examples show how reactions between umbilic points on a variable surface can be related to higher order umbilic catastrophes.

1. Introduction

When light passes through a water drop of irregular shape resting on a glass surface it focuses to produce a system of caustic surfaces. In a previous paper (Nye 1978) the water drop lens was taken to be thin, and small enough in its vertical dimension for gravity to have a negligible effect on its shape. This is a good approximation for a drop, a few millimetres across, resting on a horizontal and moderately clean glass plate; but drops of water clinging to an inclined or vertical surface, such as raindrops on a window pane, are often significantly distorted by gravity. We study in this paper how gravity modifies the caustics.

Without gravity the caustics produced generically in the three-dimensional image space are all the elementary catastrophes of appropriate codimension, with the exception of the hyperbolic umbilic: the fold, cusp, swallowtail and elliptic umbilic. Gravity allows the hyperbolic umbilic to appear generically.

In spite of the natural irregularities of any drop, the caustic singularities that it produces, the system of focal surfaces, have a remarkable degree of organisation. The main result of the paper is to show that part of this organization can be understood by regarding the parabolic umbilic (D_5) and the symbolic umbilic (E_6), which are higher-dimensional catastrophes, as organizing centres. This can be demonstrated by so manipulating a drop that its surface contains degenerate umbilic points corresponding to these higher singularities. In a natural drop the degeneracy is removed and it is found that some of the caustic patterns can be understood as unfoldings of D_5 and E_6. In addition we find in the experiments that the local structure of E_6 is accompanied by a characteristic topological feature, part of the global pattern, and this must mean that a still higher order organising centre is at work. This is probably the double cusp, whose topology is at present only partially understood (Zeeman 1977, Poston & Stewart 1978).

The main part of the paper confines itself to an approximation which is valid for thin inclined drops when the surface tension is sufficiently large. When this approximation does not hold, as for thicker drops under gravity on a horizontal surface, one sees yet another range of caustic patterns, strikingly different from those shown here and only resolvable under high magnification. They will be discussed elsewhere; some of them can be shown to be organized by the double cusp, denoted by Arnol'd (1975, p. 31) as X_9 or alternatively as $X_{1,0}$, and by the higher catastrophe $Y^1_{2,2}$.

Umbilic points on the surface of a drop are stable features: they are not destroyed by a small perturbation. However, they can pass from one class to another and can also undergo reactions by encounter with other umbilic points. We show by example in §6 how umbilic reactions on a surface, which are associated with degenerate umbilic points, can be related to umbilic catastrophes.

2. Observation

If a distant source of light is viewed through a water drop on a vertical glass surface by placing the eye very close to the drop, one commonly sees a caustic pattern of folds and cusps like figure 1 (plate 1), the most conspicuous feature being a bright fold, convex outwards, at the top of the field of view. If the glass substrate is now rotated in its own plane, the caustic pattern does not

rotate rigidly but continuously reorganizes itself in such a way that the bright convex fold remains at the top of the field. Thus we are certainly dealing with an effect of gravity, and evidently it is the top part of the drop, which refracts the light downwards, that is responsible. In thin drops that are not subject to gravity it is known (Berry 1976) that the folds must always be concave outwards.

A very similar picture is frequently seen if one examines the field very close to the drop with a low-power microscope. A conspicuous bright fold again appears, often convex outwards, but this time it comes from the lower part of the drop (figure 2*a*, plate 1). Within the fold can be seen several diffraction stars, each of which represents an elliptic umbilic focus (Berry, Nye & Wright 1979). These diffraction patterns are indistinguishable from those corresponding to focal sections, but they are very insensitive to the focusing control of the microscope and so we should not conclude that the plane of the figure actually passes through the elliptic umbilic foci.

In figure 2*b* the plane of focus of the microscope has been brought closer to the drop; the star-shaped diffraction patterns have moved downwards through the fold and each has produced a cusp. The sequence, which involves piercing, beak-to-beak and swallowtail events concealed by diffraction, is part of the unfolding of the parabolic umbilic (diagrams 10–16 and 1 of figure 7). When an elliptic umbilic focus lies exactly on the fold we have the parabolic singularity itself. The transition shown in figure 2*a*, *b* is typical in the near field. (The appearance in figure 2*b* of the faint stars outside each cusp shows that closer still to the drop the process shown in figure 6 (*d*)–(*a*) of Nye (1978) will occur.)

In the far field of random drops patterns similar to figure 2*a* (but inverted) are commonly seen with the naked eye. In this case the transition from 2*a* to 2*b* can be produced by tilting the glass substrate out of the vertical; it can also be accomplished dynamically by giving the drop a slight movement (as can be verified when walking in the rain, wearing spectacles and viewing a distant light; at each pace the elliptic umbilic stars pierce the fold in striking unison).

A further way of producing the transition is to rotate the substrate in its own plane. Then the whole pattern rotates, but as each cusp approaches the top it retracts by the transition 2*b* to 2*a* and thus allows the bright fold at the top to remain convex and uncusped. Continuing the rotation, and following the diffraction star into which a particular cusp has transformed, one sees it move first towards the image of the point source (formed by light which has passed outside the drop) and then away again, always pointing one radial spoke towards the source. Then it pierces the bright fold again on the other side of the vertical and becomes once more a cusp. In this way one can follow any given cusp-star through 360° as it rotates with the substrate. In figure 1 a procession of such diffraction stars can be seen above the direct beam; each one would become a cusp on rotation.

The broad explanation of this behaviour is as follows. The effect of gravity is to make the drop pendulous so that its surface slope, relative to the vertical substrate, is small at the top and larger at the bottom. Accordingly, rays which pass through the peripheral zone of the drop are refracted weakly at the top and more strongly at the bottom. Now the irregularities in the edge of the drop produce many umbilic points in the drop surface in this peripheral zone. They are elliptic rather than hyperbolic because here the rapidly varying local form of the surface is governed primarily by surface tension rather than by gravity (which gives only a slowly varying pressure). Near the top edge where the pressure, and hence the total curvature, is least the umbilic points focus far from the drop and so are seen as diffraction stars in the far field. (The umbilic points near the bottom edge focus much nearer the drop, as we have seen: a simple consequence of the higher

pressure.) Thus in the far field the complicated peripheral zone of the drop gives strongly refracted cusps from the lower part and weakly refracted stars from the upper part, arranged as in figure 1. In a crude approximation the cusp-star locus is a gradient mapping of the peripheral zone.

Considering the top part of the drop surface and moving radially inwards along a vertical line, after passing through the peripheral zone a point of inflexion is encountered, where the radial curvature is zero, and this maps into the central point of the bright convex fold. More generally the caustic in the far field comes from the line of zero Gaussian curvature on the drop surface (Berry 1976); in the top half of the drop the main branch of this locus lies inside the peripheral zone of elliptic umbilics.

As the vertical substrate is rotated in its own plane the edge of the drop remains fixed to it, but of course the shape of the surface of the drop must change because of gravity. However, the main effect of rotation, so far as the peripheral zone is concerned, is merely to change the overall slope of the surface; detailed features in the peripheral curvature pattern evidently rotate, to a good approximation, with the substrate, and each elliptic umbilic point in this region thus maintains its position. (Since they all have index $-\frac{1}{2}$ (§6) they could not in any case interact and lose their identities.)

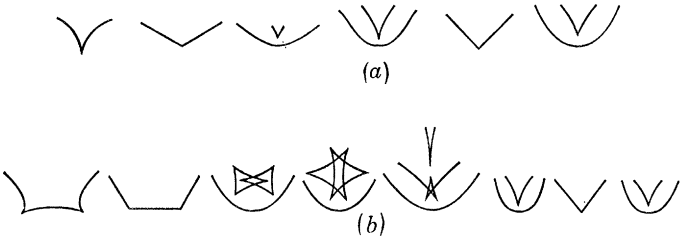

FIGURE 3. Two symmetrical focusing sequences starting near the drop and moving away. (*a*) starts with a single cusp and (*b*) starts with two.

Let us return to the near field of a random drop as seen in the microscope and consider the effect of changing the plane of focus. Very close to the drop the caustic figure resembles the outline of the drop itself, but with cusps associated with salients in the outline (Nye 1978). As the plane of focus recedes the cusps from the bottom of the drop retract, as we have discussed; there follows a complex sequence of interactions between the various parts of the caustic, and notably between the many elliptic umbilic patterns as they unfold.

To reduce the complexity and help show up systematic features the following experiment was done. A piece of opaque tape was stuck to a glass slide, a circular or oval hole was cut in the tape and a drop of water from a hypodermic syringe was placed to span the hole. Although the perimeter of the drop was now fixed, the drop shape could be varied by tilting the slide, by rotating it in its own plane, by putting in more water, or by allowing the drop to evaporate slowly. The slide, placed vertically, was illuminated with a horizontal, broadened laser beam and the region just beyond the water drop lens was viewed with a microscope.

With this arrangement the same features are seen as have already been described, cusps being produced from irregularities in the hole (the result of imperfect cutting), but now, as the plane of focus recedes, two systematic modes of unfolding can be distinguished, both involving the parabolic umbilic. (*a*) If the drop is rotated so that the caustic close to its plane has a cusp at the bottom, the focusing sequence (figure 3*a*) goes near a parabolic umbilic (second diagram, as already discussed) and then through a hyperbolic umbilic. The near-parabolic umbilic can be one of many in the field, but there is only one visible hyperbolic umbilic and it dominates the

field (figure 4*a–d*, plate 2). It is always at or near the orientation shown and it contrives to maintain this attitude even when the hole is rotated. It persists into the far field where it appears, partially unfolded, as a conspicuous feature placed centrally at the bottom of the field (the naked eye sees it in the virtual field at the top; the outer fold is the usual prominent one, convex outwards, and the cusp fits in below it). (*b*) If the drop is rotated so that two cusps lie symmetrically at the bottom of the field, the focusing sequence (figure 3*b*) goes near to two parabolic umbilics (second diagram) followed by the mutual piercing of two curvilinear triangles, a beak-to-beak event, a butterfly and a hyperbolic umbilic, which then dominates the whole field. Since it is essentially invariant to rotation of the hole it is the 'same' hyperbolic umbilic as was seen in (*a*). (Figure 14*a*, *b* and *d–f*, made not with a round hole but with one having a flat side at the bottom, shows the first part of such a sequence.)

Thus the two different symmetrical starting configurations produce the same final pattern, the single hyperbolic umbilic. We shall see (§ 4) that the first characteristic sequence is to be associated with the parabolic umbilic (D_5) and the second (§ 5) with the symbolic umbilic (E_6), but that global topology is involved as well as the local unfolding of these two singularities. We have remarked that the natural irregularities in the edge of the drop produce many umbilic points in the drop surface close to the edge. However, nearer the centre of the drop the effect of the boundary irregularities is damped out and the caustics from this area, where gravity is important and which gives the single hyperbolic umbilic focus, behave much more systematically.

Having once recognized this systematic behaviour with round and oval holes it was possible to go back to drops of uncontrolled outline and see that at least some of the apparent complexity of the unfoldings could be understood in terms of the two basic sequences (*a*) and (*b*).

3. Theory

What sort of umbilic foci would we expect theoretically? Consider a water drop of general outline under the combined forces of surface tension and gravity, resting on an inclined plane glass plate (figure 5*a*, *b*). With origin in the surface of the drop take rectangular cartesian axes with $O\bar{z}$ as the inward normal to the surface, $O\bar{y}$ horizontal and $O\bar{x}$ (tangential to the drop) positive downwards. A beam of parallel light is incident on the lower surface of the drop in such a direction that, after refraction through the glass substrate, the rays are parallel to $O\bar{z}$. Thus, within the drop, the incident wavefronts are plane and parallel to the upper surface of the drop at the origin, and we can now forget about the lower surface of the drop and the substrate. We wish to calculate the shape of the wavefronts after refraction at the upper surface.

Within the drop the excess pressure $\bar{p}$ satisfies

$$\operatorname{grad}\bar{p} = \rho\boldsymbol{g}, \quad \boldsymbol{g} = (g\sin\theta, 0, g\cos\theta),$$

where g is the gravitational acceleration, θ is the angle of $O\bar{x}$ below the horizontal ($0 < \theta < \pi$) and ρ is the density. Therefore, at the drop surface

$$\bar{p} = \bar{p}_0 + \rho g(\bar{x}\sin\theta + \bar{h}\cos\theta),$$

where $\bar{p}_0$ is the excess pressure in the water at O, and $\bar{h}(\bar{x}, \bar{y})$ is the perpendicular distance of the surface below the $(\bar{x}, \bar{y})$ plane. In the approximation $|\operatorname{grad}\bar{h}| \ll 1$ the surface tension T then imposes the condition

$$\frac{\partial^2\bar{h}}{\partial\bar{x}^2} + \frac{\partial^2\bar{h}}{\partial\bar{y}^2} = \frac{\bar{p}_0}{T} + \frac{\rho g}{T}(\bar{x}\sin\theta + \bar{h}\cos\theta). \tag{1}$$

We shall study the regime where the last term in this equation is negligible. Physically this corresponds to having the surface tension sufficiently large: if $\bar{p}_0, \rho, g$ and θ are held fixed while T is increased, eventually $\bar{h}$ is proportional to T^{-1}, and so the last term becomes proportional to T^{-2} and may be neglected. Keeping $\bar{p}_0$ fixed while T increases means that the curvature $\nabla^2\bar{h}$ *decreases* and so the analysis applies to 'thin' drops. (Notice that what might seem the more obvious procedure of allowing g to become small gets rid of both the $\bar{x}$ and the $\bar{h}$ terms together and we lose all effect of gravity.) The wavefront just above the drop has the form

$$\bar{f} = (n-1)\,\bar{h}, \tag{2}$$

where $\bar{f}(x, y)$ is its perpendicular height above the $(\bar{x}, \bar{y})$ plane, and n is the refractive index.

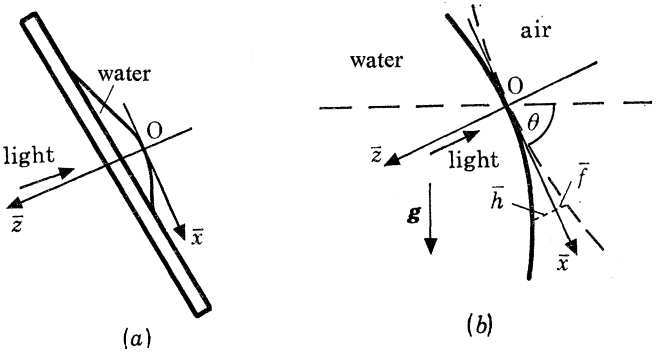

FIGURE 5. (*a*) Coordinate system. (*b*) $\bar{h}(\bar{x}, \bar{y})$ defines the drop surface (full curve); $\bar{f}(\bar{x}, \bar{y})$ defines the wavefront (broken curve).

Inserting this in (1), defining a length $l_0 = \{T/(n-1)\,\rho g \sin\theta\}^{\frac{1}{2}}$ and transforming to dimensionless coordinates x, y, z, dimensionless wavefront height f, and dimensionless pressure excess p_0 given by

$$\bar{x} = l_0 x, \quad \bar{y} = l_0 y, \quad \bar{z} = l_0 z, \quad \bar{f} = l_0 f, \quad \bar{p}_0 = \rho g l_0 \sin\theta\,.p_0, \tag{3}$$

we obtain the governing differential equation

$$\frac{\partial^2 f}{\partial x^2} + \frac{\partial^2 f}{\partial y^2} = p_0 + x. \tag{4}$$

Note that, since $\bar{h} = \{l_0/(n-1)\}f$, $f(x, y)$ can be thought of equally well as giving the shape of the wavefront $\bar{f}$ or of the drop itself $\bar{h}$.

The general solution of (4) with O an umbilic point is

$$f = \tfrac{1}{4}p_0(x^2+y^2) + \tfrac{1}{2}xy^2 + F(x, y), \tag{5}$$

the complementary function $F(x, y)$ being harmonic and of order 3 or higher. For the present we restrict attention to solutions symmetric in y. Then the solution near O is the power series

$$f = \tfrac{1}{4}p_0(x^2+y^2) + \tfrac{1}{6}\alpha x^3 + \tfrac{1}{2}(1-\alpha)\,xy^2 + q(x^4 - 6x^2y^2 + y^4) + O(5), \tag{6}$$

where α and q are arbitrary constants. Whether O is elliptic or hyperbolic depends on the cubic terms and specifically (Berry & Hannay 1977) on the sign of the discriminant

$$D = 4\alpha(\alpha-1)^3; \quad \left.\begin{array}{l} D > 0 \text{ elliptic,} \\ D < 0 \text{ hyperbolic.} \end{array}\right\} \tag{7}$$

Thus there are two critical values of α, 0 and 1, where the umbilic point changes its character (figure 6). We can guess, and will shortly prove, that $\alpha = 0$ represents a parabolic umbilic (D_5), but $\alpha = 1$ is a triple root and so gives warning that it may give something more singular. We shall see that this root represents the symbolic umbilic (E_6). To study the limit $\theta \to 0$ one keeps $\sin\theta$ out of the scaling so that (4) becomes

$$\nabla^2 f = p_0 + x\sin\theta,$$

and the factor $(1-\alpha)$ in (6) becomes $(\sin\theta - \alpha)$. Thus the roots are now at $\alpha = 0$ and $\sin\theta$. As $\theta \to 0$ the hyperbolic region in figure 6 disappears: horizontal (non-degenerate) umbilic points are always elliptic.

The wavefront must now be related to a generating function ϕ. For a general point in the image

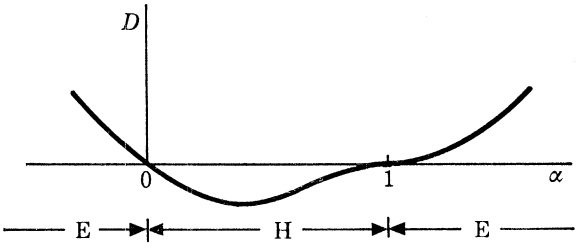

FIGURE 6. The catastrophe discriminant D as a function of the parameter α which governs the drop shape.

space beyond the drop we use coordinates $(X, Y, Z) = (x, y, -z)$. If $\boldsymbol{R} = (X, Y)$ and $\boldsymbol{r} = (x, y)$, the (non-dimensional) distance l between a general point $(\boldsymbol{r}, f)$ on the wavefront and a general point $\mathrm{P} = (\boldsymbol{R}, Z)$ in the image space beyond it is given by

$$l^2 = (\boldsymbol{R} - \boldsymbol{r})^2 + (Z - f(\boldsymbol{r}))^2. \tag{8}$$

To define ϕ discard the part of l^2 that does not depend on $\boldsymbol{r}$ and divide the remainder by $-2Z$; thus define

$$\phi(\boldsymbol{r}; \boldsymbol{R}, Z) = f(\boldsymbol{r}) - \frac{\boldsymbol{r}^2}{2Z} + \frac{\boldsymbol{r}.\boldsymbol{R}}{Z} - \frac{\{f(\boldsymbol{r})\}^2}{2Z}. \tag{9}$$

Keeping $\mathrm{P} = (\boldsymbol{R}, Z)$ fixed and varying $\boldsymbol{r}$ the condition for ϕ to be stationary, $\nabla_r \phi = 0$, implies

$$\nabla f(\boldsymbol{r}) = (\boldsymbol{r} - \boldsymbol{R})/(Z - f). \tag{10}$$

This equation is satisfied exactly on a normal from P to the wavefront, that is, on a ray through P. Thus the stationary condition on ϕ defined by (9) generates the rays. The rays provide a mapping from the three-dimensional space beyond the wavefront, the control space (X, Y, Z), into the two-dimensional space (x, y), the state space, of the wavefront itself. The caustics we are studying are the envelopes of the rays, their focal surfaces; they constitute the singularities in control space of a gradient mapping. Mathematically they are catastrophes (Thom 1975, Berry 1976, Poston & Stewart 1978, Nye 1978).

If we use equation (9) for the generating function there are no approximations. However, for most of the work we shall use the simpler form

$$\phi(\boldsymbol{r}; \boldsymbol{R}, Z) = f(\boldsymbol{r}) - \frac{\boldsymbol{r}^2}{2Z} + \frac{\boldsymbol{r}.\boldsymbol{R}}{Z} \tag{11}$$

constructed by omitting the term in f^2, which generates

$$\nabla f(\boldsymbol{r}) = (\boldsymbol{r} - \boldsymbol{R})/Z. \tag{12}$$

Equation (12) describes the rays within the approximation $f \ll Z$; we shall discuss the effect of this approximation in more detail later.

In this paper we are mainly concerned with solutions of equation (4) in the form of expansions about umbilic points. We do not try to fit the solutions to the boundary conditions on the edge of the drop, except for one example, due to Dr M. V. Berry, which we now describe. This is the following exact solution of (4) for a drop with a circular perimeter:

$$f = \tfrac{1}{4}p_0(x^2+y^2) + \tfrac{1}{8}x(x^2+y^2-k^2). \tag{13}$$

On the circle $x^2+y^2 = k^2$ the height of the wavefront f takes the constant value $\frac{1}{4}p_0k^2$. Thus there exists a plane $\bar{z}$ = constant which cuts the drop in a circle, as required.

The surface described by (13) has a non-zero slope at O, and O is umbilic. Thus although the umbilic focus is off-axis the umbilic point on the surface is at the centre of the drop. The cubic terms correspond to $\alpha = \frac{3}{4}$ in equation (6) and therefore the umbilic point is hyperbolic. Without gravity the drop would be a spherical cap and the caustic would be an isolated point, which is structurally unstable. Gravity is enough to remove the indeterminacy and produce a structurally stable hyperbolic umbilic focus.

To examine this focus first insert the wavefront (13) into equation (11) to obtain ϕ. Move the origin in control space to the focus $(\frac{1}{4}k^2/p_0, 0, 2/p_0)$, defining the new control variables

$$X_1 = X - \tfrac{1}{4}k^2/p_0, \quad Z_1 = Z - 2/p_0;$$

then, dropping nonlinear terms in the control variables, we have for the generating function

$$\phi = \tfrac{1}{8}x(x^2+y^2) + \tfrac{1}{8}p_0^2 Z_1(x^2+y^2) + \tfrac{1}{2}p_0(xX_1 + yY).$$

We will consider the plane through the focus $Z_1 = 0$. The critical points of ϕ, given by $\nabla_r \phi = 0$, provide the ray mapping

$$\left.\begin{aligned} 4p_0 X_1 &= -3x^2 - y^2, \\ 2p_0 Y &= -xy. \end{aligned}\right\} \tag{14}$$

The set of degenerate critical points of ϕ, whose locus in (X_1, Y) is the caustic, is obtained by imposing the further condition that the Hessian determinant of ϕ with respect to the state variables (x, y), namely $\phi_{xx}\phi_{yy} - \phi_{xy}^2$, be zero. We therefore have

$$3x^2 = y^2 \quad \text{or} \quad y = \pm\sqrt{3}\,x,$$

which, when combined with (14), gives

$$X_1 = \pm\sqrt{3}\,Y,$$

Description of plate 1

Figure 1. Caustic figure from a water drop on a vertical surface as it would be seen by eye in the far field. (The concentric diffraction rings are due to imperfections in the optical system.)

Figure 2. Caustics formed by the lower part of a drop in the near field (inversion by the microscope has been removed). (*a*) and (*b*) are from an irregular drop; (*c*) and (*d*) are from a drop in an imperfect circular hole. (*a*) is further from the drop than (*b*). (*c*) is further from the drop than (*d*). The transitions are organized by the parabolic umbilic.

(1)

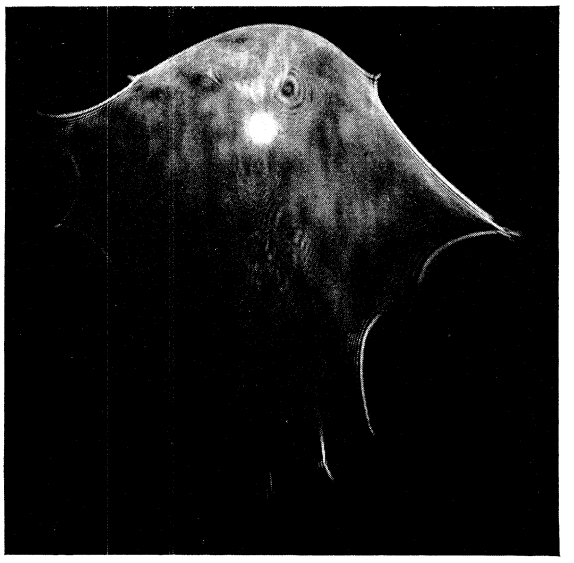

(2*a*)

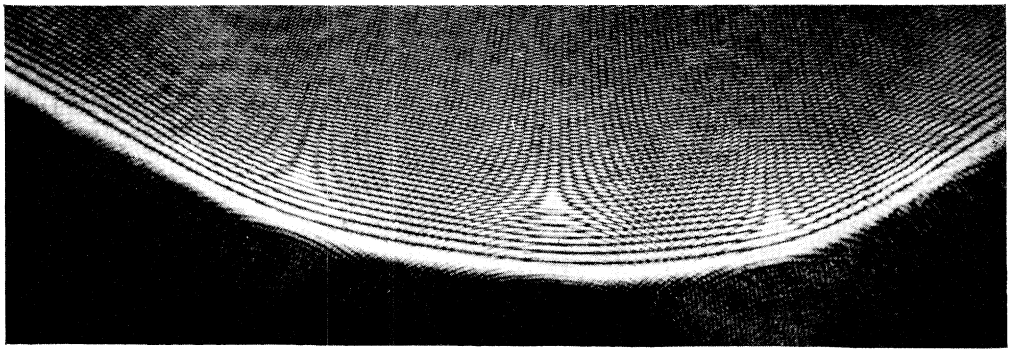

(2*b*)

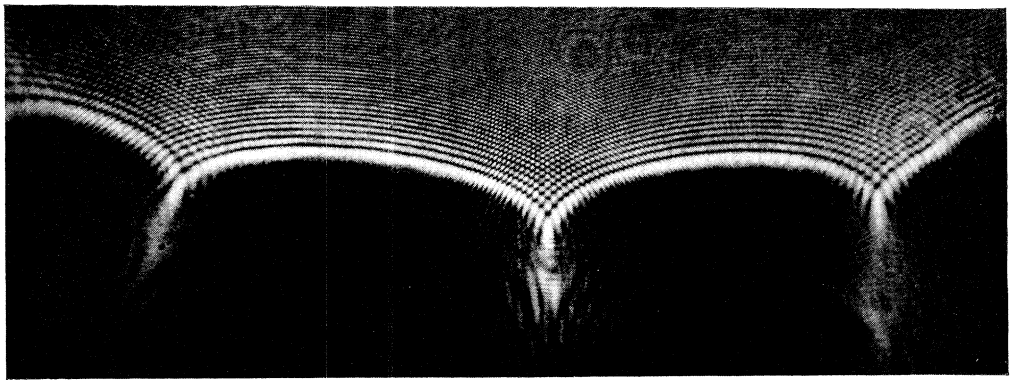

(2*c*)

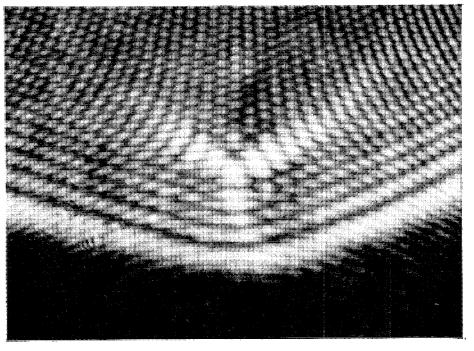

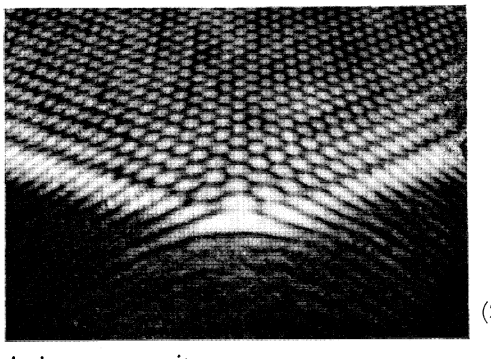

(2*d*)

FIGURES 1 AND 2. For description see opposite.

(*Facing p.* 32)

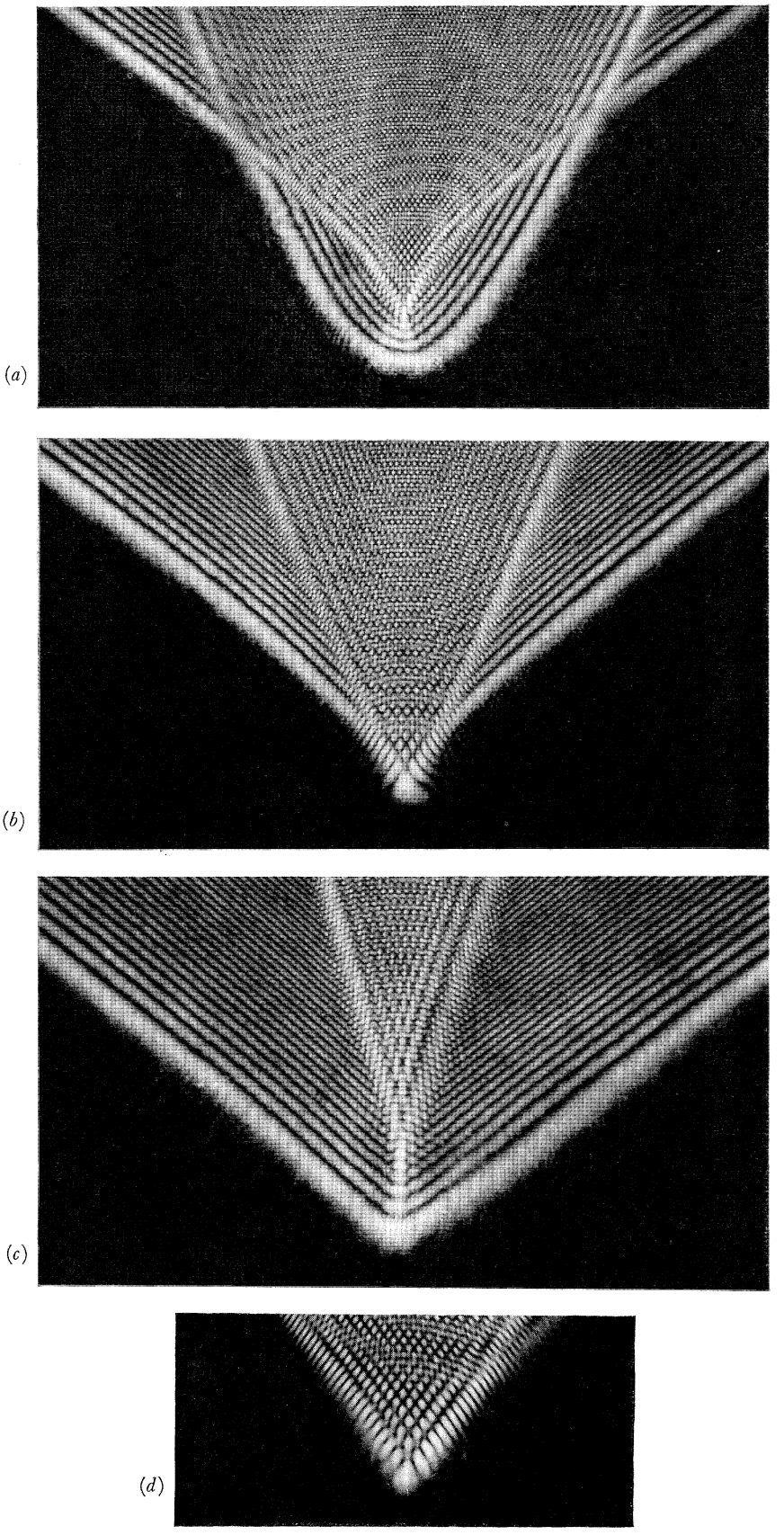

FIGURE 4. (*a*)–(*c*) Sequence through a hyperbolic umbilic focus, and (*d*) the singular section for a different drop. The edge of the drop was fixed by a circular hole, 5.5 mm in diameter, held vertically.

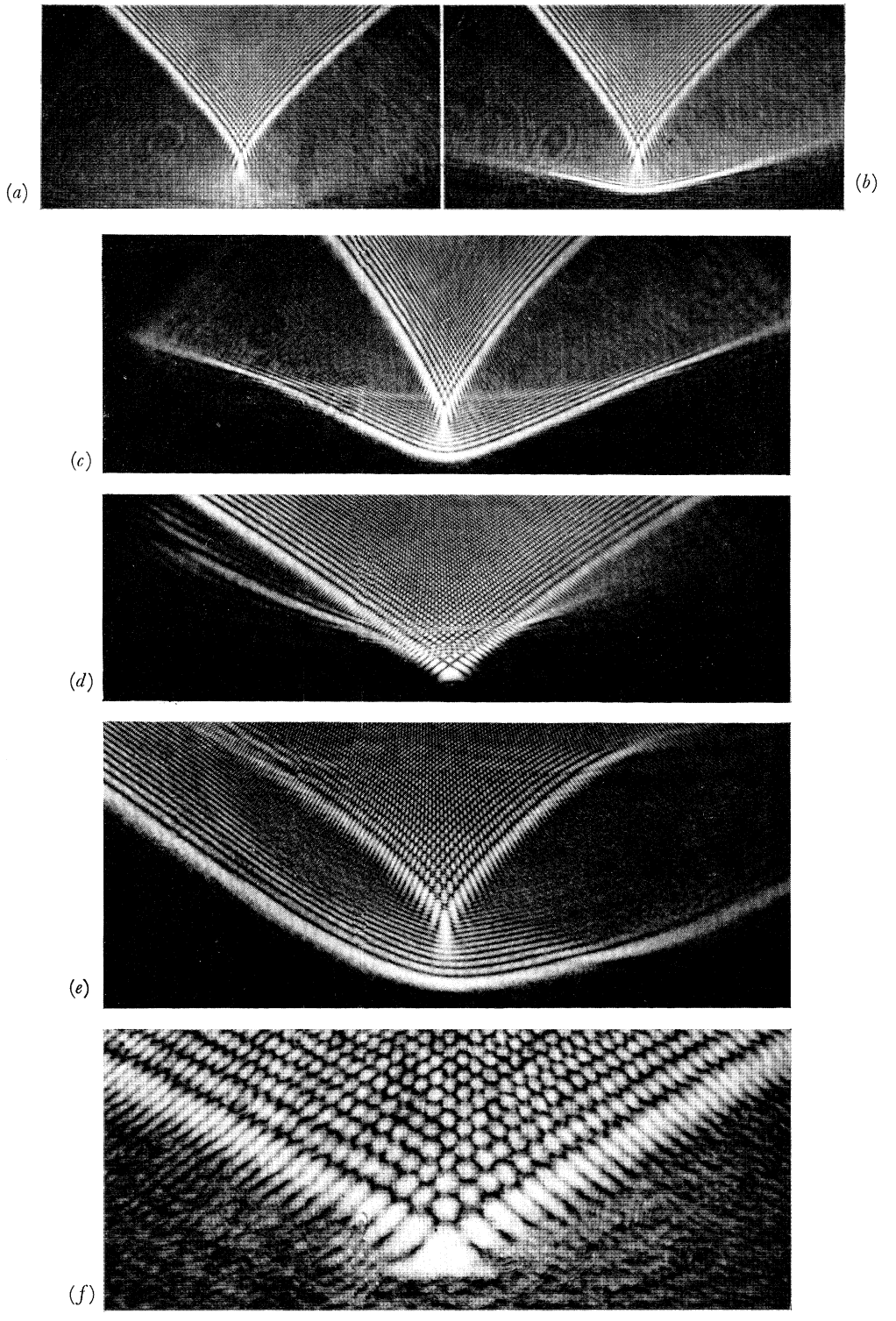

FIGURE 8. Light caustics near a parabolic umbilic focus. (*a*)–(*e*) correspond to the left hand half of figure 7. (*f*) is a section almost through the singularity itself.

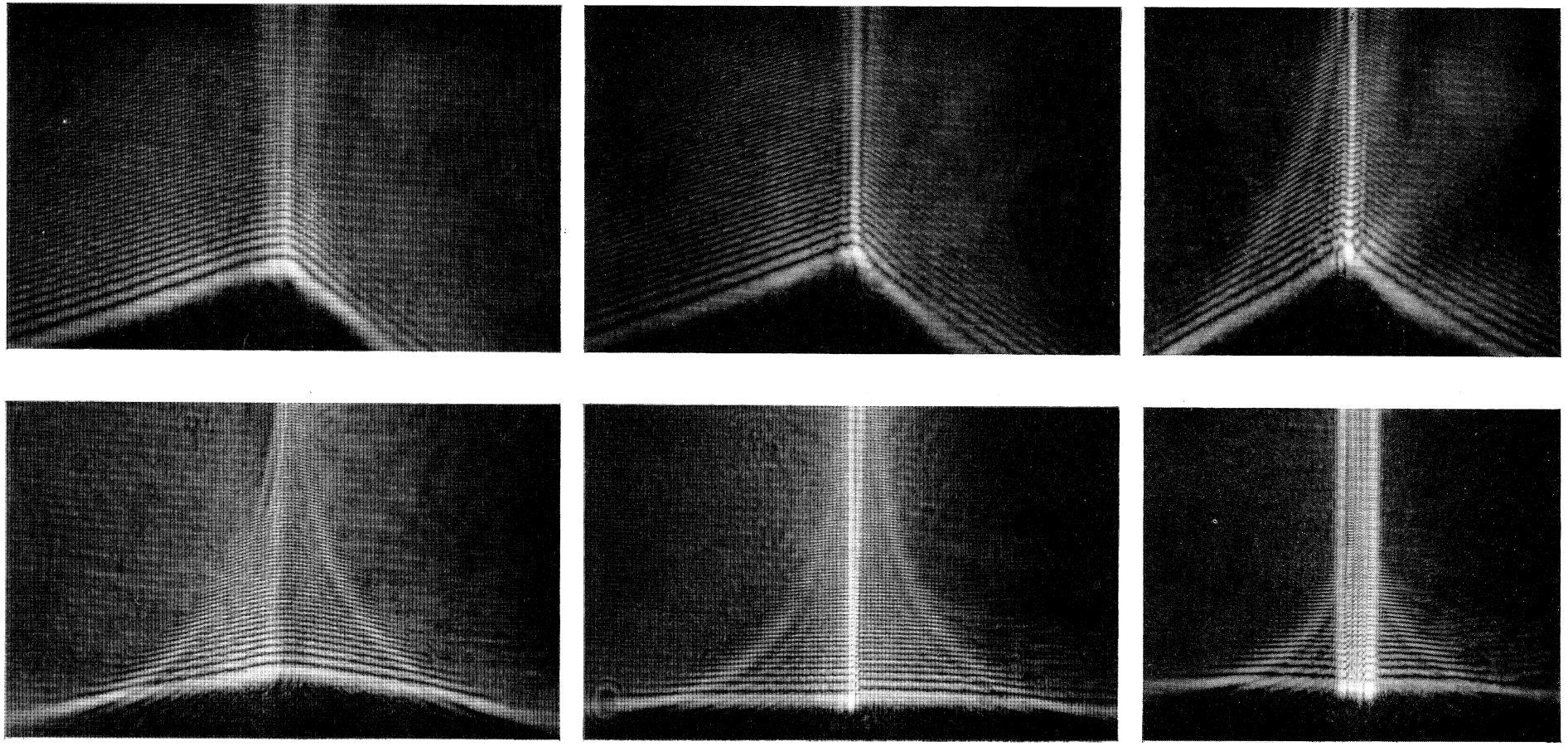

(11*a*) 9, 10 (11*b*) 5–10 (11*c*) 5–10

(12*a*) 11 (12*b*) (12*c*) 1

FIGURE 11. Unfoldings of E_6 with $c = 0$, e positive and very near the origin. (*a*), (*b*) and (*c*) are all from the same drop and show the effect of moving the plane of focus of the microscope towards the drop. Substrate at 30° to horizontal. Numbers shown refer to diagrams in figure 9.

FIGURE 12. Unfoldings of E_6 with $c = e = 0$. In (*a*) to (*c*) the plane of focus of the microscope has been moved towards the drop. (*a*) d negative; (*b*) $d = 0$, singular section; (*c*) d positive.

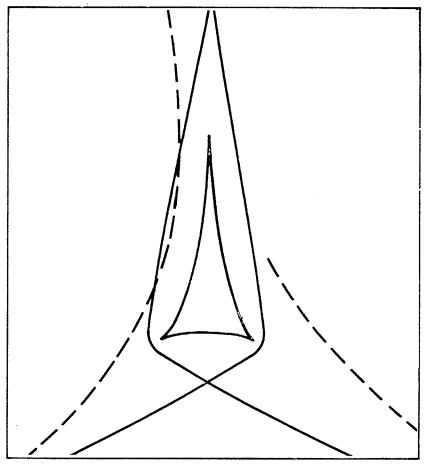

(*a*) 2

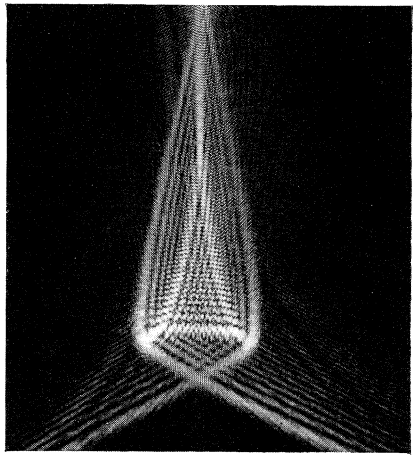

(*f*) 3

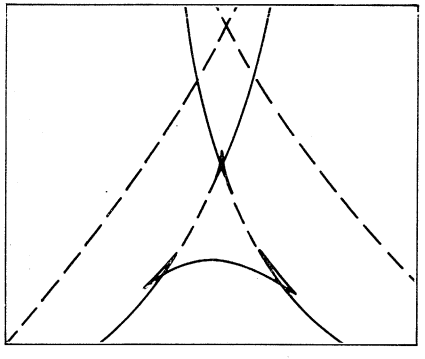

(*b*) 6

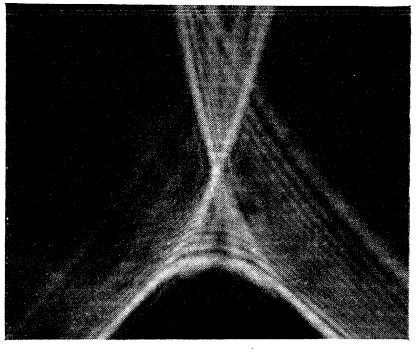

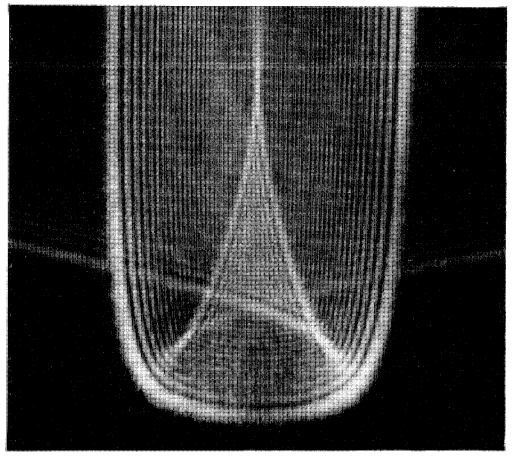

(*e*) 16

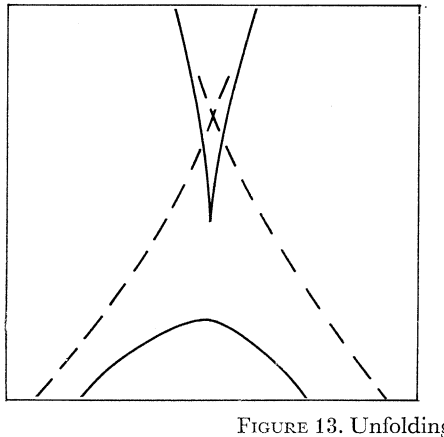

(*c*) 10

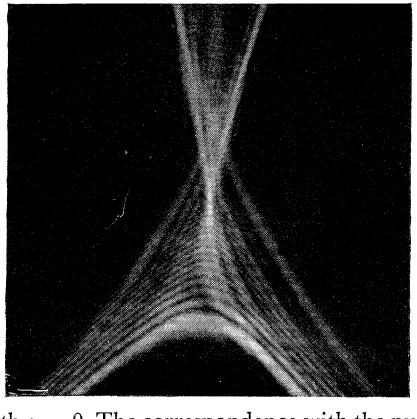

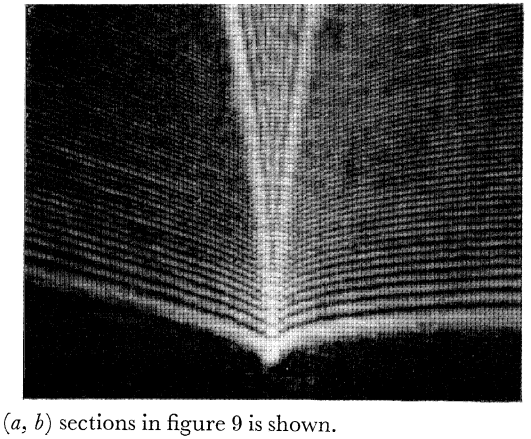

(*d*) 13

FIGURE 13. Unfoldings of E_6 with $c = 0$. The correspondence with the numbered (a, b) sections in figure 9 is shown.

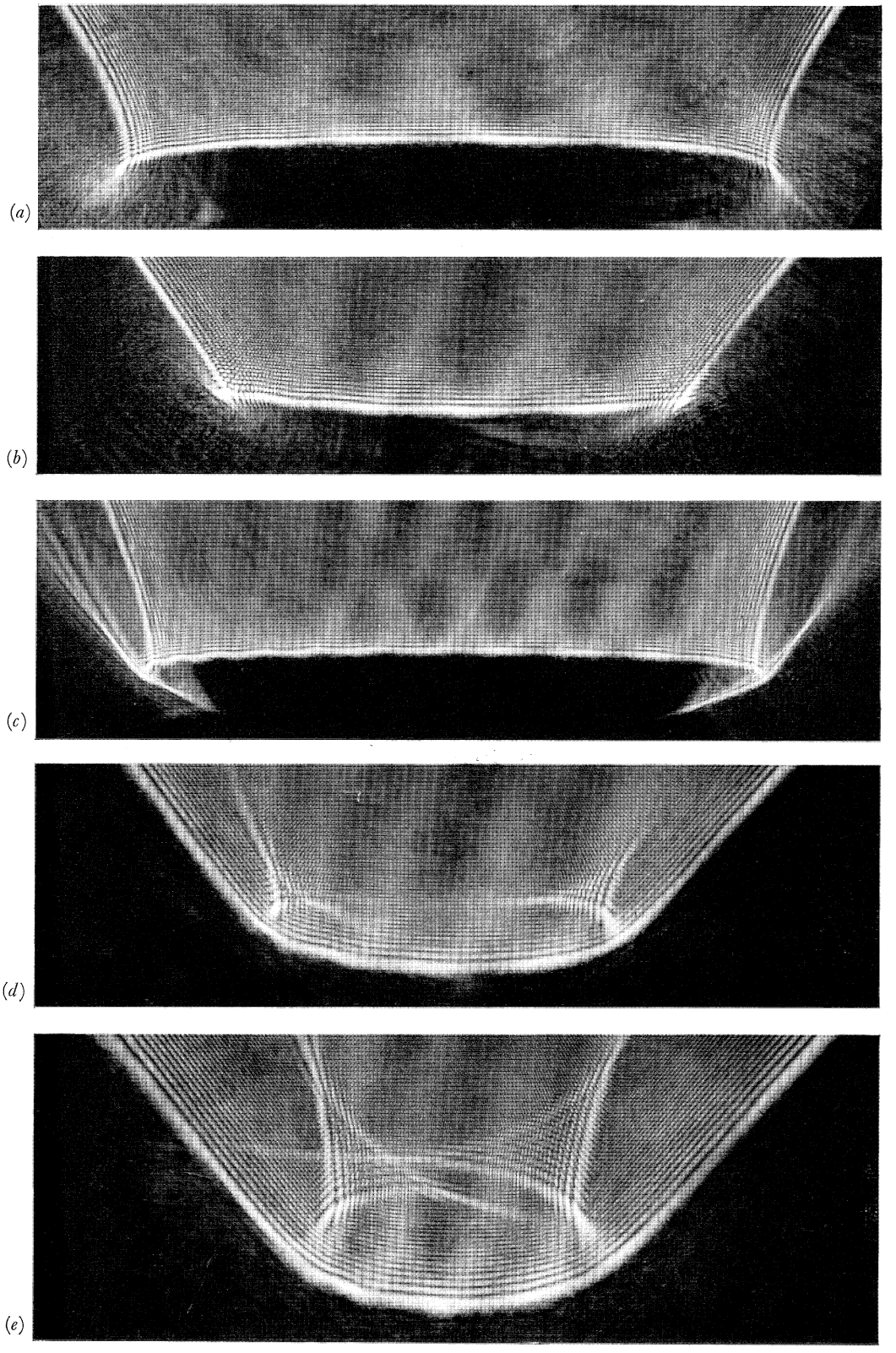

FIGURES 14(*a*)–(*e*). For description see opposite.

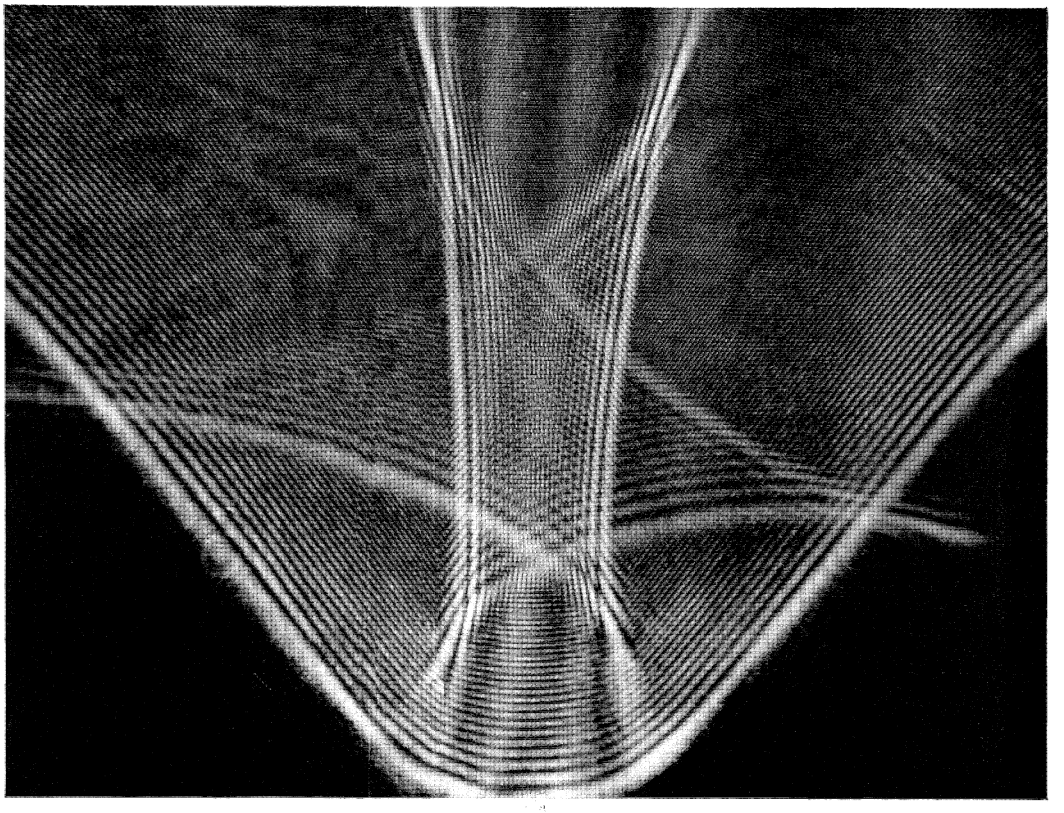

(*f*)

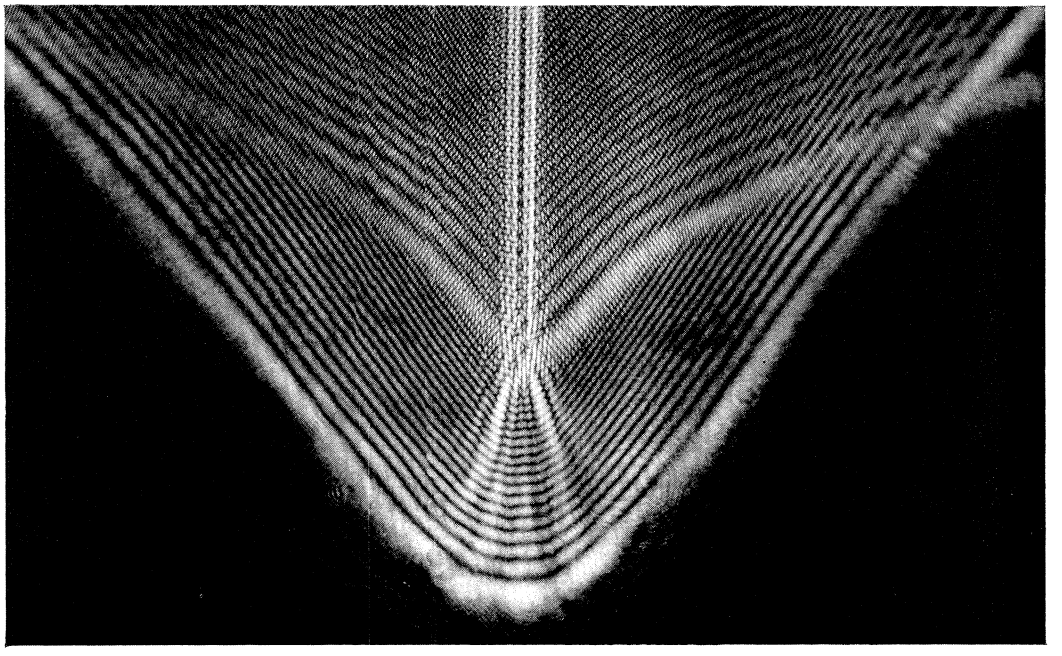

(*g*)

FIGURE 14. (*a*)–(*b*) and (*d*)–(*f*) is a focusing sequence moving away from the drop showing at (*b*) two simultaneous parabolic umbilics as part of the non-local unfolding of E_6. (*c*) is from another drop and shows lips unfolding from (*b*).

(15)

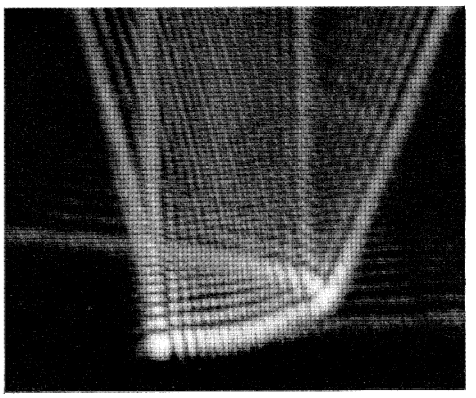

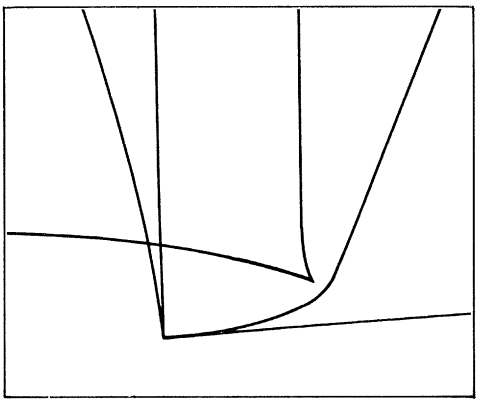

(17*a*)

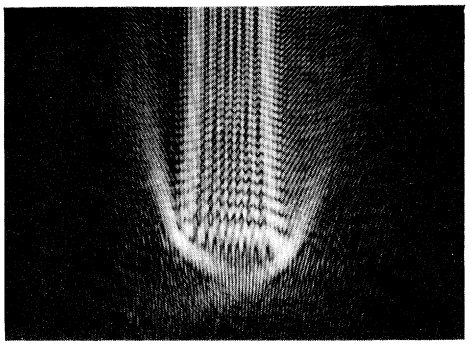

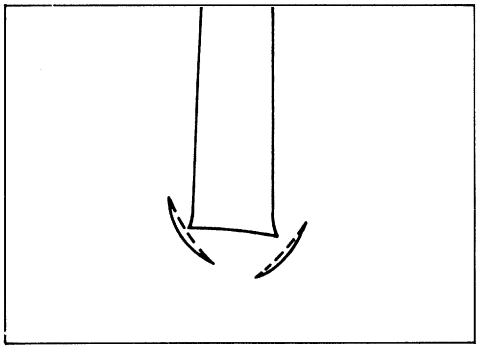

(17*b*)

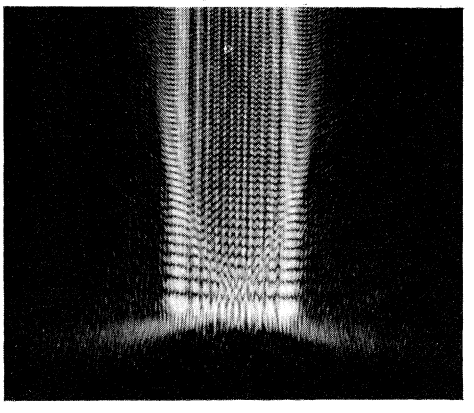

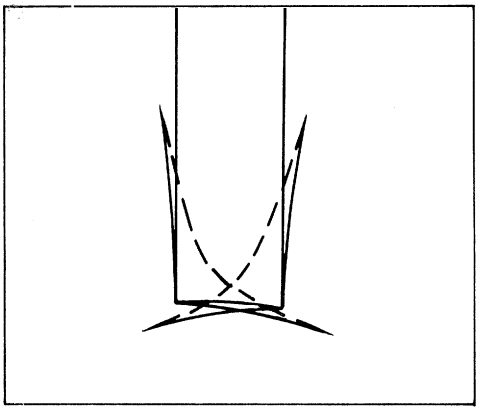

(17*c*)

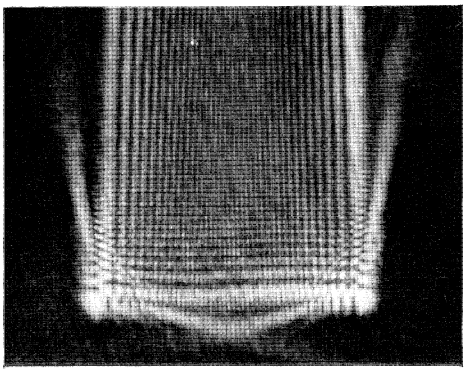

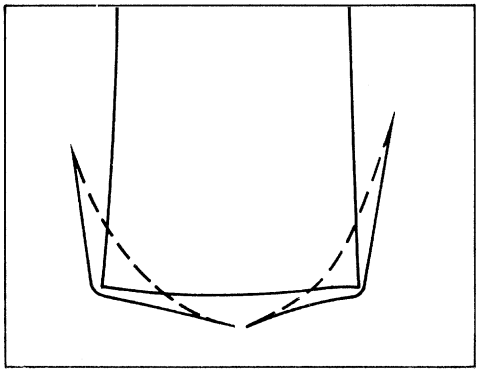

FIGURE 15. Unfolding of E_6 with $c \neq 0$.

FIGURE 17. Unfoldings of E_6 disguised by the proximity of D_5 loci.

with the restriction $X_1 \leqslant 0$ (since p_0 is positive). Thus the caustic in the focal plane is a V-shape with arms at 60°.

This model of the circular drop provides the explanation for the observations in § 2 where drops in imperfect oval and circular holes produced a conspicuous hyperbolic umbilic focus. The arms of the V in figures 4*b* and *d* do indeed come together at an angle not significantly different from 60°. A very good example appears in fig. 8 of the paper by Tanner (1978); his optical geometry is different from ours but equivalent.

4. The parabolic umbilic (D_5)

To study the parabolic umbilic we use the wavefront (6) and obtain ϕ from equation (11). Since the umbilic focus is at $(0, 0, 2/p_0)$, define the focusing control variable as before by $Z_1 = Z - 2/p_0$. We need keep only terms up to $O(4)$ in f. Then, keeping only the linear terms in the control variables, we have for the generating function

$$\phi = \tfrac{1}{2}xy^2 + \alpha(\tfrac{1}{6}x^3 - \tfrac{1}{2}xy^2) + q(x^4 - 6x^2y^2 + y^4) + \tfrac{1}{8}p_0^2 Z_1(x^2 + y^2) + \tfrac{1}{2}p_0(Xx + Yy). \tag{15}$$

A standard form for the parabolic umbilic and its universal unfolding is (Poston & Stewart 1978, p. 122; Thom 1975, p. 84)

$$\pm (x'^2 y + \tfrac{1}{4}y'^4 + tx'^2 + wy'^2 - ux' - vy'), \tag{16}$$

where x', y' are state variables and t, w, u, v are controls. This suggests that the parameters q and α governing the shape of the wavefront should be treated differently. Whereas q is a non-zero constant, α will now be regarded as a control variable and will be thought of as small.

To bring (15) into the standard form (16) we look first at the germ, obtained by setting $\alpha = X = Y = Z_1 = 0$, namely

$$\tfrac{1}{2}xy^2 + q(x^4 - 6x^2y^2 + y^4), \tag{17}$$

and use the rules of equivalence. x^2y^2 may be neglected in comparison with xy^2. Then, introducing the new state variable x_1, where

$$x_1 = x + 2qy^2,$$

consider the expression

$$\tfrac{1}{2}x_1 y^2 + qx_1^4 = \tfrac{1}{2}xy^2 + qy^4 + qx^4 + \text{terms in } x^3y^2, \quad x^2y^4, \quad xy^6, \quad y^8.$$

Since the terms in the last group are all negligible compared with xy^2 or y^4, the germ (17) reduces to $\frac{1}{2}x_1 y^2 + qx_1^4$ which, with appropriate scaling factors, becomes the standard form

$$\pm (x'^2 y' + \tfrac{1}{4}y'^4). \tag{18}$$

The lower sign results if $q < 0$, in which case we reverse the sign of x_1. Thus we have shown that (17) and (18) are equivalent.

With state variables x_1, y, (15) now takes the form

$$\phi = \tfrac{1}{2}x_1 y^2 + qx_1^4 + \alpha(\tfrac{1}{6}x_1^3 + qy^4 + \tfrac{4}{3}q^3y^6) + \tfrac{1}{8}p_0^2 Z_1(x_1^2 + y^2 + 4q^2y^4) + \tfrac{1}{2}p_0 X(x_1 - 2qy^2) + \tfrac{1}{2}p_0 Yy, \tag{19}$$

where we have dropped terms in $\alpha x_1^2 y^2$, $\alpha x_1 y^4$, $\alpha x_1 y^2$, $Z_1 x_1 y^2$ which are small compared with $x_1 y^2$ in the germ. The transformation

$$x_2 = x_1 + A + By^2 + Cy^4$$

with

$$A = \tfrac{1}{24}\alpha/q, \quad B = 2q(\alpha + \tfrac{1}{2}p_0^2 Z_1 q), \quad C = \tfrac{8}{3}q^3\alpha$$

removes the terms in αx_1^3, αy^4 and αy^6; then, dropping terms in $x_2^3 y^2$ and $x_2^3 y^4$, and also terms quadratic or higher in the control variables X, Y, Z_1, α leaves

$$\phi = \tfrac{1}{2}x_2 y^2 + q x_2^4 + \tfrac{1}{8}p_0^2 Z_1 x_2^2 + (-\tfrac{1}{48}\alpha/q + \tfrac{1}{8}p_0^2 Z_1 - p_0 qX)\, y^2 + \tfrac{1}{2}p_0 X x_2 + \tfrac{1}{2}p_0 Y y. \qquad (20)$$

Comparing this with the standard form (16) we can now relate the physical controls X, Y, Z_1, α to the standard controls t, w, u, v (table 1). Thus, while u, v, w are simply proportional to Y, X and Z_1, t is a linear combination of α, Z_1 and X.

TABLE 1. VARIABLES FOR THE PARABOLIC UMBILIC (D_5)

Thom (1975)	this experiment
x'	$2^{-\frac{3}{4}}Q^{-1}y$
y'	$\pm 2^{\frac{1}{2}}Q^2 x_2$
t	$\pm 2^{\frac{3}{2}}Q^2(-\frac{1}{48}\alpha/q + \frac{1}{8}p_0^2 Z_1 - p_0 qX)$
w	$\pm 2^{-4}Q^{-4}p_0^2 Z_1$
u	$\mp 2^{-\frac{1}{4}}Q p_0 Y$
v	$-2^{-\frac{3}{2}}Q^{-2}p_0 X$

$Q = (\pm q)^{\frac{1}{8}}$, and where there is a choice the upper sign is for q positive and the lower for q negative.

Before discussing these connections any further let us review the status of the physical controls. With a given drop (X, Y, Z_1) represents the variable observation point; on the other hand p_0, α and q depend on the shape of the drop. We can think of it like this. A drop is created, symmetrical in y, and the origin is taken at an umbilic point. An umbilic focus will then appear at $X = Y = Z_1 = 0$. It will be elliptic or hyperbolic and it will unfold in the observation plane (X, Y) as the focusing control Z_1 is changed. p_0, α and q will be non-zero. Now, by alteration of one external parameter, the shape of the drop is slightly changed, but keeping it symmetrical in y and not changing the position or the orientation of the umbilic point (the umbilic point, being structurally stable, will not disappear). p_0, α and q will now have different values, and the umbilic focus will be at a different Z. If the external parameter is correctly chosen we may be able to arrange that α passes through zero. Then the umbilic point on the drop will change from elliptic to hyperbolic, or vice versa, and at $\alpha = 0$ it will be parabolic.

The theoretical argument we have used involves not only the cubic but also the quartic terms in the expansion of the wave surface about the umbilic point. This raises an issue that needs further discussion, because the original differential equation is only approximate, and therefore one may legitimately ask whether the higher-order terms in its solutions have any physical meaning.

There are three relevant approximations, all connected with paraxiality: (*a*) use of the expression $\nabla^2\bar{h}$ in equation (1) for the curvature of the drop; (*b*) equation (2) which connects the form of the wavefront with that of the drop effectively linearizes Snell's law; (*c*) the generating function (11) with the omission of the term $\frac{1}{2}f^2/Z$ gives the rays only approximately (equation (12)). For each of these approximations the expansion about the umbilic point is correct up to cubic terms only. We argue as follows. Equation (5) is an exact solution of equation (4). Therefore our analysis of the caustics is correct for an imaginary system whose wavefronts exactly obey the governing differential equation (4) and whose rays exactly obey equation (12). The real system is slightly different, but, because the singularities we are concerned with, the catastrophes, are structurally stable in the space of the available control parameters (four for the parabolic umbilic), the difference between the real and the imaginary system will merely move them in control

space; it will not destroy them or change their topology. More specifically we assume that the difference from the calculated form does not move a singularity so far that it interacts with another. The structural stability of the singularities is essential to the result.

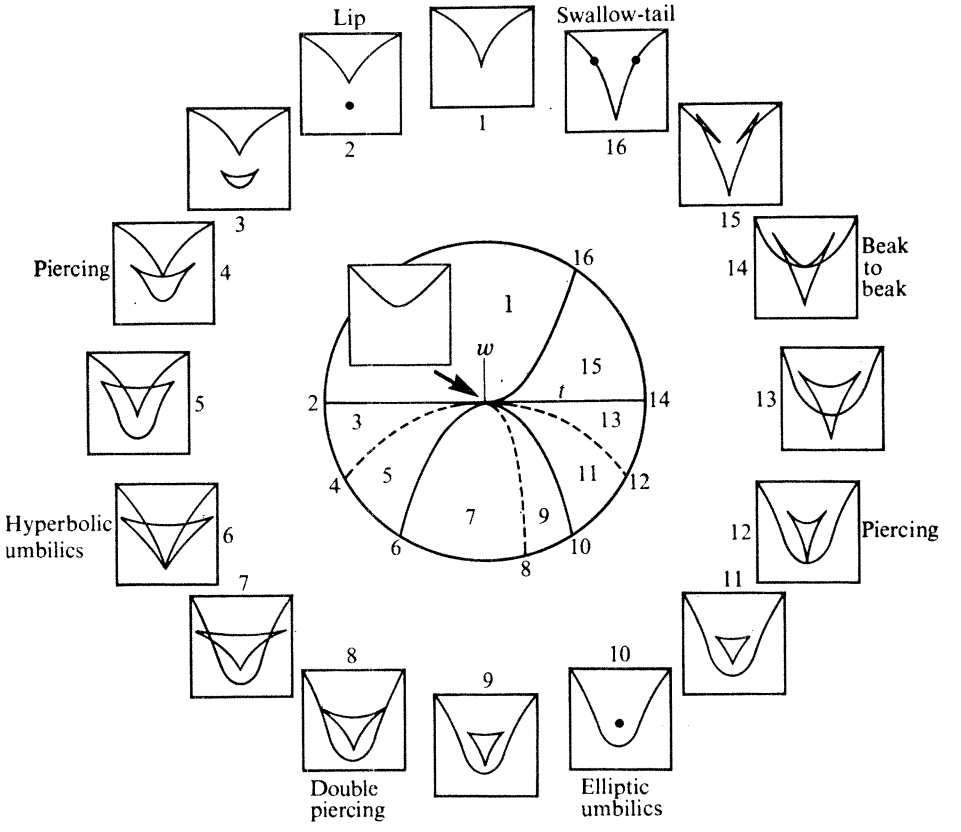

FIGURE 7. Unfoldings of the parabolic umbilic (D_5). Reproduced from *Structural Stability and Morphogenesis*, 1975, written by René Thom (translated from the first French edition by D. H. Fowler), with the permission of the publishers, Addison–Wesley, Advanced Book Program, Reading, Mass., U.S.A.

4.1 *Observation of* D_5

Figure 7, taken from Thom's book (1975, p. 86), illustrates the universal unfolding of the parabolic umbilic (D_5) as a clock diagram. For points on a unit circle in the (w, t) plane it shows the corresponding sections (u, v). To realise these unfoldings physically the hole-in-tape method was used. The main controls on the shape of the drop were changing the shape of the hole and charging up the drop with more water; changing the tilt of the whole apparatus with the glass substrate near vertical made only a small difference. A V-shaped hole was chosen so that close to the drop there was a single cusp at the bottom of the field. Figures 8*a–e* (plate 3) show the effect of moving the plane of focus away from the drop (some evaporation occurred between *c* and *d*), *b* is the lips event; *d* is the hyperbolic umbilic; *f*, from a different drop, is a section through the parabolic umbilic singularity itself. The photographs of figure 8 correspond to the left hand half of figure 7.

The right hand half of the clock diagram provides sequences whose details are masked in these experiments by diffraction. The transition from figure 2*b* to 2*a*, where a cusp retracts to leave a smooth fold and a singular section of an elliptic umbilic, is one example. Figures 2*c*, *d*, two members of a focusing sequence, are another. The three-rayed diffraction pattern seen in

figure 2*c* above the fold represents a non-singular section of the elliptic umbilic (Berry, Nye & Wright 1979) (diagram 9 or 11 in figure 7). Figure 2*d* is closer still to the parabolic umbilic centre and the diffraction pattern can be seen as intermediate between those of figure 2*a* and that of figure 8*f*; in fact the hat shaped central maximum gives a good way of recognizing the parabolic umbilic.

The detailed relation of the photographs to the theoretical sections is more complicated than might at first be thought from the fairly simple connection between X, Y, Z_1, α and u, v, t, w shown in table 1. Note, for example, that although X and Z_1 are simply proportional to v and w the X and Z_1 axes are inclined to the v and w axes. A typical photograph represents a plane $Z_1 =$ constant, $\alpha =$ constant. In the space (u, v, t, w) this is not quite the plane $t =$ constant, $w =$ constant shown by a typical member of the clock diagram. Note also that a change of focus Z_1 alters not only w but also t. Increasing Z_1 is observed to correspond to decreasing w; therefore, the lower sign in table 1 applies and q must be negative. Hence in a (t, w) projection, such as figure 7 (central diagram), increasing Z_1 carries a point from upper right to lower left. Thus in figure 18 note that a line near $\alpha = 0$ passes first near the parabolic umbilic centre and then cuts the hyperbolic umbilic locus 6, which is consistent with the sequence of figure 3*a*.

5. The symbolic umbilic (E_6)

We now examine the second critical value of α seen in figure 6, $\alpha = 1$. Take for the wavefront $f(x, y)$ the same form (6) as before, but because we wish to be able to break the symmetry in y we add the lowest order term that will do this, ϵxy, where ϵ is a constant. With the new parameter γ defined as $1-\alpha$ the wavefront, up to quartic terms, is then

$$f = \tfrac{1}{4}p_0(x^2+y^2) + \epsilon xy + \tfrac{1}{6}(1-\gamma)\,x^3 + \tfrac{1}{2}\gamma xy^2 + q(x^4 - 6x^2y^2 + y^4). \tag{21}$$

Notice that unless $\epsilon = 0$ the origin is no longer an umbilic point. The generating function ϕ defined by (11) becomes

$$\phi = \tfrac{1}{6}x^3 + q(x^4 - 6x^2y^2 + y^4) + \epsilon xy + \gamma(\tfrac{1}{2}xy^2 - \tfrac{1}{6}x^3) + \tfrac{1}{8}p_0^2 Z_1(x^2+y^2) + \tfrac{1}{2}p_0(Xx + Yy). \tag{22}$$

A standard form for the symbolic umbilic (E_6) and its universal unfolding is (Poston & Stewart 1978, p. 122; Callahan 1977, p. 9)

$$\pm\,(x'^3 + y'^4 - ex'y'^2 - dy'^2 - cx'y' - by' - ax'), \tag{23}$$

with x', y' as state variables and a, b, c, d, e as controls. This suggests that of the coefficients p_0, q, ϵ, γ appearing in the wavefront, p_0 and q should be thought of as constants, with ϵ and γ as small parameters playing the part of controls.

In the germ
$$\tfrac{1}{6}x^3 + q(x^4 - 6x^2y^2 + y^4) \tag{24}$$
x^4 is small compared with x^3. Then introduction of the new state variable

$$x_1 = x - 12qy^2$$

and neglecting x_1y^4, $x_1^2y^4$ and y^6 in comparison with y^4 removes the term in x^2y^2 to leave

$$\tfrac{1}{6}x_1^3 + qy^4, \tag{25}$$

which with appropriate scaling factors is the germ of E_6,

$$\pm\,(x'^3 + y'^4). \tag{26}$$

(If q is negative we change the sign of x_1 and obtain the lower sign.) Thus (24) is equivalent to (26).

Coming to the unfolding part, (22) now has the form

$$\phi = \tfrac{1}{6}x_1^3 + qy^4 + \epsilon x_1 y + (\tfrac{1}{2}\gamma + 3p_0^2 qZ_1)\, x_1 y^2 + 12q\epsilon y^3 + \tfrac{1}{8}p_0^2 Z_1 x_1^2 + (\tfrac{1}{8}p_0^2 Z_1 + 6p_0 qX)\, y^2 + \tfrac{1}{2}p_0 Xx_1 + \tfrac{1}{2}p_0 Yy,$$

where terms in γx_1^3, γy^4, $\gamma x_1 y^4$, γy^6, $Z_1 y^4$ have been omitted as negligible compared with those in the germ, and $\gamma x_1^2 y^2$ as negligible compared with $\gamma x_1 y^2$.

To remove the terms in x_1^2 and y^3 respectively put

$$x_2 = x_1 + \tfrac{1}{4}p_0^2 Z_1$$

and

$$y_1 = y + 3\epsilon,$$

neglecting terms quadratic or higher in the controls, to give

$$\phi = \tfrac{1}{6}x_2^3 + qy_1^4 + (\tfrac{1}{2}\gamma + 3p_0^2 qZ_1)\, x_2 y_1^2 + (\tfrac{1}{8}p_0^2 Z_1 + 6p_0 qX)\, y_1^2 + \epsilon x_2 y_1 + \tfrac{1}{2}p_0 Yy_1 + \tfrac{1}{2}p_0 Xx_2. \quad (27)$$

This is now in the standard form (23) and the physical controls X, Y, Z_1, γ, ϵ may therefore be related to a, b, c, d, e as listed in table 2.

TABLE 2. VARIABLES FOR THE SYMBOLIC UMBILIC (E_6)

Callahan (1977)	this experiment
x'	$\pm 6^{-\frac{1}{3}}x_2$
y'	$Q^2 y_1$
a	$-\tfrac{1}{2}.6^{\frac{1}{3}}p_0 X$
b	$\mp\tfrac{1}{2}Q^{-2}p_0 Y$
c	$-6^{\frac{1}{3}}Q^{-2}\epsilon$
d	$\mp Q^{-4}(\tfrac{1}{8}p_0^2 Z_1 + 6p_0 qX)$
e	$-6^{\frac{1}{3}}Q^{-4}(\tfrac{1}{2}\gamma + 3p_0^2 qZ_1)$

$Q = (\pm q)^{\frac{1}{8}}$ and where there is a choice the upper sign is for q positive and the lower for q negative.

If ϵ is kept zero the origin is always umbilic. As with the parabolic umbilic, starting with a drop symmetrical in y, we have to imagine a single external parameter changed in such a way that the position and orientation of the umbilic point is unaltered, the drop shape remaining symmetrical in y throughout. p_0, q and γ will change, and if we can make the range of variation such that it includes $\gamma = 0$ the umbilic point at the origin will pass from hyperbolic to elliptic via E_6. We discuss later (§6) what this means in terms of the drop surface. An essential difference from the parabolic umbilic is the extra control variable ϵ which corresponds to breaking the symmetry in y. Just as with the parabolic umbilic, we appeal to the structural stability of E_6 to establish the essential correctness of the quartic terms in the expansion of the wavefront.

5.1. *Observation and discussion of* E_6

As table 2 shows, the canonical pattern in the space a, b, c, d, e is distorted in the physical control space. Crudely speaking, however, (a, b) represents the plane of observation (X, Y), d is mainly influenced by focusing (Z_1), while e is mainly governed by charging the drop and by changing the shape and size of its symmetrical boundary. The control c which breaks the symmetry about the vertical plane is conveniently handled by rotating the microscope stage, and hence the drop, in its own plane.

Figure 9 shows the theoretical sections in the (a, b) plane that result from varying d and e while keeping $c = 0$; the figure is taken from Callahan (1977), but the extra folds shown by broken lines have been added on the basis of the present observations. It will be seen that at the T-shaped most singular section, at $d = e = 0$, these extra folds do not pass through the origin, the T-junction, and so they are not an essential part of the unfolding of E_6, but rather part of the global pattern in which it happens to be embedded in these experiments. As one moves along the positive d axis from the origin (figure 10) the extra folds (often rather dim) cause the horizontal arms of the central T-shape to disappear; unless this is recognized the frequent absence of these arms, as in figure 10*d*, can be puzzling. The extra folds naturally play a part, not essential to E_6 but potentially confusing, in all the other observed unfolding patterns.

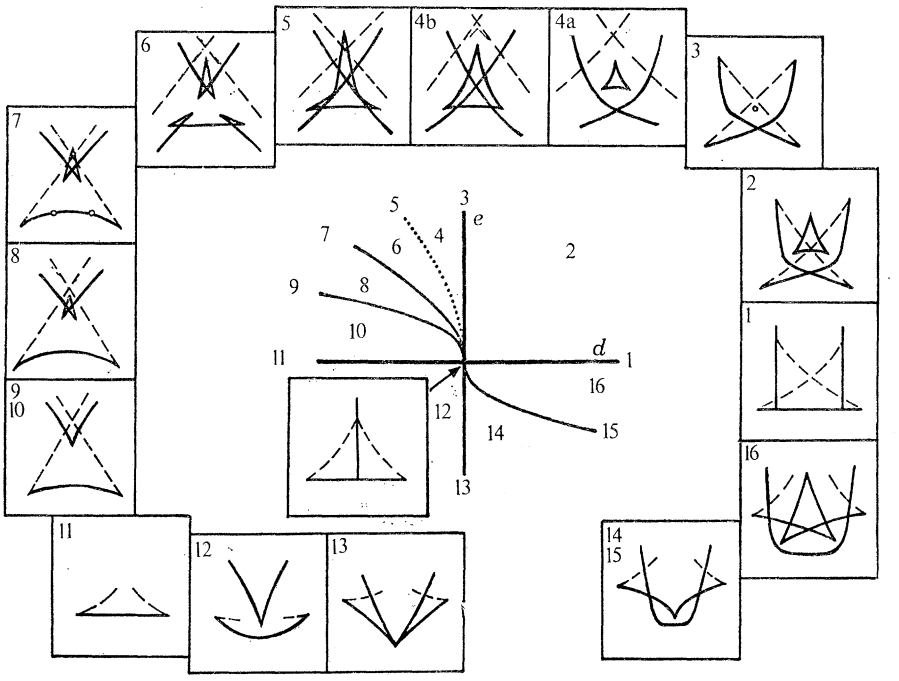

FIGURE 9. Unfoldings of the symbolic umbilic (E_6), based on Callahan (1977). Each diagram is an (a, b) section corresponding to $c = 0$ and the (d, e) value indicated in the centre.

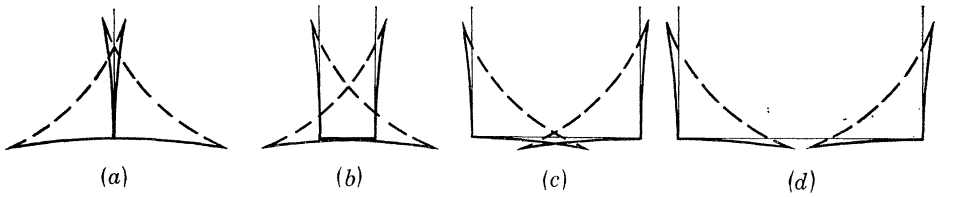

FIGURE 10. Global modification to E_6 caused by extra folds (broken lines). Patterns (a)–(d) correspond to moving along the d axis from the origin.

The photographs in figure 12 (plate 4) correspond with the diagrams in figure 9 with $e = 0$. They were obtained by the same technique as for D_5, except that a hole shape was chosen that would give at the bottom of the field close to the drop two cusps symmetrically placed (figure 3*b*) rather than a single central one. A symmetrical hole about 2 mm wide with a flat side at the bottom rather than a corner is essentially what is needed. One has to be sure that the microscope aperture is not cutting off any high-angle rays; this often dictates a high-power objective, and for

the same reason it helps to have easy control of the angle of the incident beam. Figure 13*a–f* (plate 5) correspond to members of the clock diagram in figure 9 with $e \neq 0$. In figure 11 (plate 4) we are in the top left quadrant of the (d, e) projection and very close to the origin. Rotating the microscope stage to make e non-zero produces patterns such as figure 15 (plate 8) which can be seen as an unsymmetrical unfolding of a 'triple-folded handkerchief' (fold twice and then fold back the top two layers to make a third fold parallel to the second). In this example a hyperbolic umbilic appears on the left but not on the right.

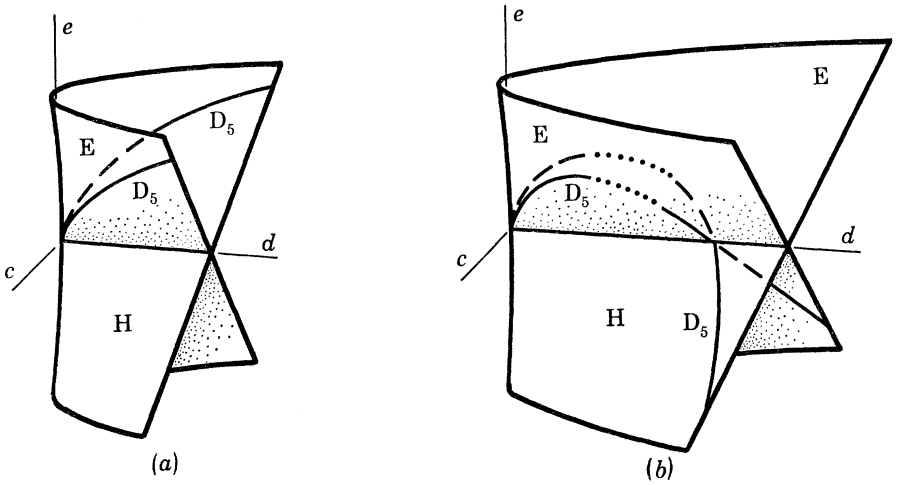

FIGURE 16. The umbilic locus for E_6: (*a*) after Callahan (1977); (*b*) with a non-local crossing of the D_5 locus. E, elliptic; H, hyperbolic.

5.2. *Global topology near* E_6

The observations described accord with what is already known about the unfoldings of D_5 and E_6. But the extra folds seen near E_6 are a new feature showing that there is also systematic global topology in its neighbourhood to be explored. In figure 3*b*, which is a typical focusing sequence obtained with a symmetrical hole, one appears in the second diagram to pass very close to two parabolic umbilics simultaneously. This is surprising because with E_6, as figure 9 shows, there is no combination of d and e with $c = 0$ which can give two parabolic umbilics. Nevertheless, by carefully changing the shape of a drop by adding more water, a droplet at a time, it was verified that one could indeed obtain two parabolic umbilic foci in the field at the same time, symmetrically placed (figure 14*b*). Figure 14*c* is from another drop and shows how 14*b* can be unfolded to give lips. The focusing sequence through figure 14*b* is shown as figure 14*a*, *b*, *d–g* (plates 6 and 7). One does not pass exactly through E_6 but through the lower right part of the clock diagram in figure 9. However, we know that with a slight change of γ as well as Z_1 we could have reached E_6 itself.

To explain this apparently paradoxical behaviour consider the umbilic locus in the space of parameters c, d, e, which, as shown by Callahan (1977), has the form of a Whitney umbrella (figure 16*a*). If (c, d, e) lies on this surface, there will be an umbilic focus in the observation plane (a, b). The surface is divided by the parabolic umbilic locus D_5, so that points above represent elliptic umbilics and points below represent hyperbolic umbilics. Notice that along the e axis in the positive direction one has a hyperbolic changing to an elliptic umbilic, while along the d axis one has at first no umbilics and then two hyperbolic umbilics (since the two sheets cross). But with $c = 0$ one never encounters the D_5 locus, except at the origin itself. Therefore, with this

topology, there can be no non-zero setting of d and e, with $c = 0$, that will give D_5. Since two D_5's are observed at the same d, e setting (in the physical controls they differ only in Y), the D_5 locus must cross itself at some point in the d, e plane: this can only be on the line where the two umbilic sheets cross. We have therefore conjectured that the global topology is as figure 16*b*; however, Dr J. Callahan (personal communication) points out that the connections shown as dotted lines are probably not correct. The question is still under discussion. In any case the behaviour in figures 3*b* and 14 is so systematic that it must result from a higher-order organizing centre, probably the double cusp, of which E_6 is a partial unfolding.

Figure 14 shows that the extra folds, shown broken in the various diagrams, originate in the two D_5's. We can now interpret patterns like figures 17*a–c*. (plate 8). As a drop is tilted, and gravity is switched on, so to speak, one can watch the lips in figure 17*a* appearing. The pattern is like figure 14*c*. We are on the d axis in figure 17*b*, and near the d axis in figure 17*c* (compare figure 10*b* to *d*), but the E_6 unfolding is disguised by the proximity of the two D_5 loci. Such patterns are in fact the rule rather than the exception; it can be hard to load the drop sufficiently full of water to reach E_6 itself without it breaking away.

6. Umbilic reactions on the surface

Both in D_5 and E_6 three of the control parameters in the unfolding are the three dimensions of the physical space in which the optical focus is formed, while the remainder control the shape of the surface of the drop. What happens to the umbilic point on the drop itself at the origin as these shape parameters are changed?

For D_5, where there is only one parameter of evolution (which could be time), the answer is simple. We use the classification of umbilic points by Berry & Hannay (1977). As α increases through zero the umbilic point at O changes from elliptic to hyperbolic, its index (the number of revolutions of the principal axes of curvature in a circuit around O) remains $-\frac{1}{2}$, and the number of straight lines of curvature passing through it remains 3. Figure 18 shows the umbilic locus projected on to the (t, w) plane. A line of constant α (constant drop shape) has positive slope near the origin; when α is small and negative it intersects the elliptic branch ($t > 0$) near the origin, and when α is small and positive it intersects the hyperbolic branch ($t < 0$). However, as α increases still further there is the possibility of a tangency between the line of constant α and the umbilic locus, corresponding to the mutual annihilation of two hyperbolic umbilics of opposite index, $\pm\frac{1}{2}$. This is beyond the range of small α, and thus represent global topology of D_5.

It is interesting to see that the tangency is with the hyperbolic rather than the elliptic branch; since all elliptic umbilics have index $-\frac{1}{2}$ two elliptic umbilics cannot annihilate. This is an example of a restriction on the orientation of the singular set of a catastrophe in control space. The physical space (X, Y, Z_1) is a three-dimensional section ($\alpha = 0$) through the four-dimensional singularity, but only certain three-dimensional sections are allowed.

To examine the event represented by the tangency first consider the form of the wavefront, or drop, given by equation (6). As we have seen, $\alpha = 0$ gives D_5 and $\alpha = 1$ gives E_6. Noting that the index discriminant (Berry & Hannay 1977) is zero for $\alpha = \frac{1}{2}$ or 1, we put $\alpha = \frac{1}{2}$. But f given by (6) is always umbilic at the origin, and so to obtain an annihilation event we must perturb the quadratic terms, while still satisfying the differential equation (4). Therefore we write

$$f = (\tfrac{1}{4}p_0 + \epsilon_1)\,x^2 + (\tfrac{1}{4}p_0 - \epsilon_1)\,y^2 + \tfrac{1}{12}x^3 + \tfrac{1}{4}xy^2 + q(x^4 - 6x^2y^2 + y^4) + O(5). \qquad (28)$$

This form does what we need. Two hyperbolic umbilic points at $(\pm\sqrt{(-\frac{1}{6}\epsilon_1 q^{-1})}, 0)$ coalesce and annihilate at O as ϵ_1 increases through zero. Figure 19 sketches the pattern of directions of principal curvature on the surface. As ϵ_1 decreases we see, in the Berry–Hannay terminology, the twin birth of a star and a monstar. To obtain these patterns qx and qy must be kept small; the cubic terms must dominate the quartic terms. (Equation (28) also contains, as part of its global pattern for $\epsilon_1 = 0$, two extra umbilics, symmetrically placed at $(\frac{1}{48}q^{-1}, \pm\frac{1}{48}q^{-1})$ and parabolic to the first approximation.)

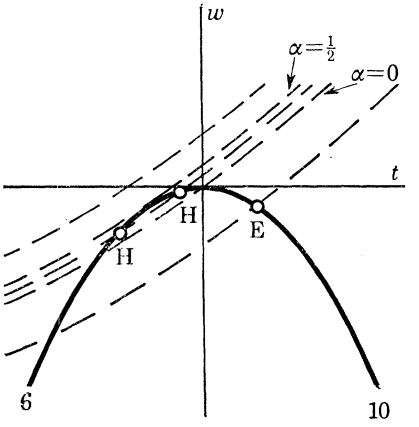

FIGURE 18. The full curve is the umbilic locus for the parabolic umbilic. The left hand branch gives hyperbolic umbilic points and the right hand branch gives elliptic umbilic points. The broken curves are lines of constant surface shape (constant α); changing the plane of focus of the microscope for a fixed drop corresponds to moving along one of these curves.

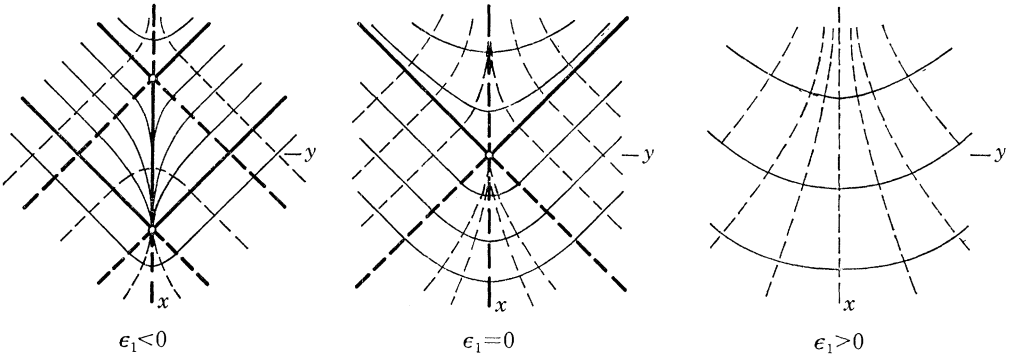

FIGURE 19. Sketch of pattern of directions of principal curvature for the mutual annihilation of two hyperbolic umbilic points on a surface. The slope ψ of the curves is given by

$$\tan 2\psi = y/[4\epsilon_1 + 24q(x^2 - y^2)].$$

Turning now to E_6 ($\alpha = 1$), there are two shape parameters $\gamma = 1 - \alpha$, and ϵ to consider. Let us preserve symmetry by keeping $\epsilon = 0$. First note from equation (21) that, as γ is changed through zero, O on the surface remains an umbilic point throughout. But we see from figure 9 that at certain settings of c and d ($e = 0$) there are two hyperbolic umbilic foci, symmetrically placed, and so at least two hyperbolic umbilic points symmetrically placed on the surface, in addition to the umbilic point at O. We do not see all three umbilic foci at once because they focus at different levels, but all the umbilic points are simultaneously present on the surface. In table 2 q is

positive (because increasing Z_1 is observed to correspond to decreasing d). So, omitting positive proportionality constants,

$$\gamma = -e+d-a.$$

For umbilics on the d and e axes $a = 0$ (Callahan 1977, p. 21). The lines of constant γ (constant drop shape) therefore run as in figure 20a, which is a section of figure 16a. As γ increases one elliptic umbilic point changes into three hyperbolic points. The index of the elliptic point must be $-\frac{1}{2}$; so by conservation of index and by symmetry the indices must be arranged as in figure 20b. As γ increases (figure 21) a single elliptic star splits into a central lemon flanked by two hyperbolic stars. (Equation (21), with $\gamma = e = 0$, contains an umbilic point at $(-\frac{1}{24}q^{-1}, 0)$ in addition to the one at the origin, but this is part of the global pattern; it could correspond to the hyperbolic umbilic caustic seen, partially unfolded, in the far field.) It is noteworthy that all three discriminants, catastrophe, index and line pattern, are zero at E_6 itself.

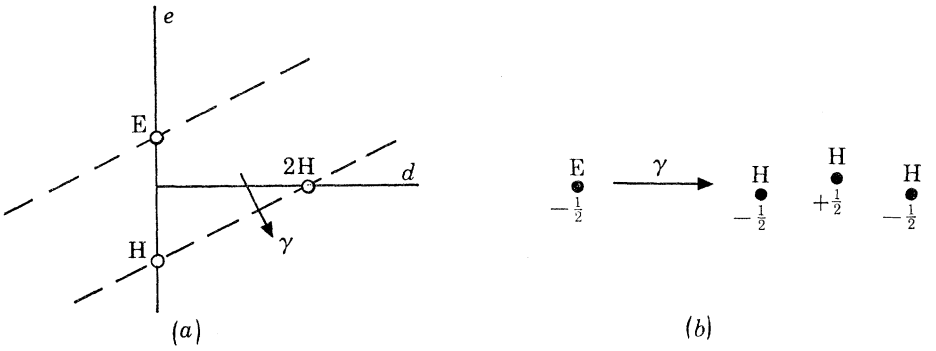

FIGURE 20. (*a*) The umbilic locus for E_6 in the (d, e) plane is the e axis (elliptic for $e > 0$, hyperbolic for $e < 0$) and the positive d axis (two hyperbolic umbilics). The broken curves are lines of constant drop shape (constant γ); changing the plane of focus carries a point along one of these curves. As γ increases a single elliptic umbilic point changes into three hyperbolic umbilic points, the indices being arranged as shown in (*b*).

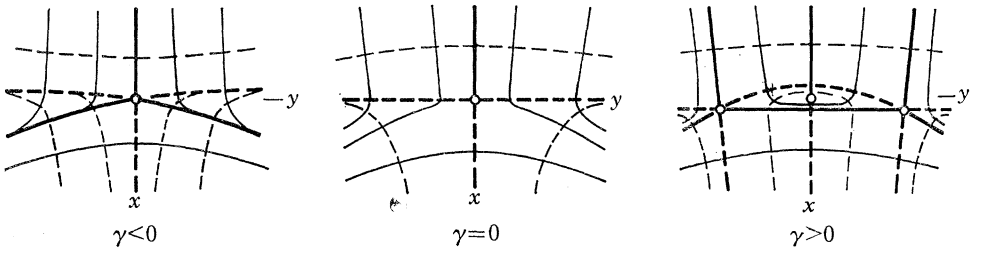

FIGURE 21. Sketch of pattern of directions of principal curvature for the E_6 umbilic reaction (symmetric case, $c = 0$). The slope, ψ, of the curves is given by $\tan 2\psi = 2y(\gamma-24qx)/(x-24qy^2)$.

These examples suggest the following conclusions. Generically, a surface will contain umbilic points. As a surface evolves with time two events involving umbilic points will occur generically: the parabolic umbilic and the creation or destruction of a pair of hyperbolic umbilics. If the evolving surface is subject to one constraint (for example, symmetry about a line) the E_6 umbilic reaction will occur generically. In a similar way each higher-order umbilic catastrophe corresponds to a family of umbilic reactions on an evolving surface. An alternative way of viewing such reactions is suggested in the appendix.

7. Further discussion

7.1. *General method*

Our theoretical treatment has depended mainly on a power series expansion of the water surface or wave surface in the immediate neighbourhood of an umbilic point. Except for the circular drop we have not considered the theoretical connection between the canonical control parameters of D_5 and E_6 and the real physical controls that change the shape of the drop (aperture size and shape, amount of water and tilt of the glass substrate) because this would have entailed finding the complete shape of the drop surface under the given physical conditions. We avoided such calculations by changing the physical controls experimentally in an intuitive way, so altering the shape parameters α or (γ, ϵ) which are effective in the immediate neighbourhood of the umbilic point, and we then connected α, γ and ϵ theoretically with the canonical controls.

The application of catastrophe theory lies in first establishing, by using the rules of equivalence, which germs we are dealing with; this enables us to deduce what controls are needed for complete unfolding, and then the theoretical notion of structural stability enables us to understand why what is seen optically is physically stable. Without that theoretical notion the stability of the observed patterns would be a mystery.

7.2 *Diffraction*

We have emphasized the geometrical optics of the observed caustic patterns, but in some of the patterns (notably those of E_6 for e positive) diffraction effects are very conspicuous. Berry (1976) has pointed out how each catastrophe has its own characteristic diffraction pattern; these are understood so far for the fold (Airy 1838), cusp (Pearcey 1946), elliptic umbilic (Trinkaus & Drepper 1977, Berry, Nye & Wright 1979) and to some extent for the swallowtail (Wright 1977) and the hyperbolic umbilic (F. J. Wright, private communication). This paper shows singular sections for the hyperbolic umbilic (rhombuses, figure 4*b*, *d*), the parabolic umbilic (hexagons, figure 8*f*) and E_6 (straight fringes, figure 12*b*).

I should like to thank Dr M. V. Berry and Dr J. Callahan, who have both kindly read a draft of this paper and commented most helpfully on it.

Appendix. Umbilic reactions

Let a smooth surface of small slope be represented by $f(x, y)$, its height above the (x, y) plane. The condition for a point to be umbilic is $f_{xx} = f_{yy}$ and $f_{xy} = 0$, where subscripts denote differentiation. So in the mapping

$$g\colon (x, y) \longrightarrow (f_{xx} - f_{yy}, f_{xy})$$

umbilic points are inverse images of the origin O′ in the target space. Since this is a mapping of the plane to the plane the only singularities that will occur generically are the fold and the cusp (Whitney 1955). If now the surface is allowed to evolve with time, when a fold of g passes through O′ the number of inverse images of O′, and therefore the number of umbilic points in (x, y), will change by two: a pair will annihilate or be created. (The other interesting event, the transition from elliptic to hyperbolic via the parabolic umbilic is not apparent in this mapping; it requires a mapping into the full jet space (f_{xx}, f_{yy}, f_{xy}) rather than into a projection of it.)

If the surface can evolve with time under the control of an additional parameter a cusp of g can be made to pass through O′. In this case three umbilic points become one or vice versa. The E_6 umbilic reaction is an example of this.

In a general map $\mathbb{R}^2 \to \mathbb{R}^2$ evolving with time the singular events are beak-to-beak, lips and swallowtail (see, e.g. Thorndike, Cooley & Nye 1978). To guide one of these events to occur at O′ needs two additional controls, making six in all (X, Y, Z plus time plus two). The beak-to-beak and lips events presumably correspond to the annihilation and creation of two E_6's; the swallowtail event presumably corresponds to a higher catastrophe of co-dimension six.

References

Airy, G. B. 1838 On the intensity of light in the neighbourhood of a caustic. *Trans. Camb. phil. Soc.* **6**, 379–403.

Arnol'd, V. I. 1975 Critical points of smooth functions and their normal forms. *Russian Math. Surveys* **30** (5), 1–75 (translated from *Uspekhi Math. Nauk* **30** (5) 3–65).

Berry, M. V. 1976 Waves and Thom's theorem. *Adv. Phys.* **25** (1), 1–26.

Berry, M. V. & Hannay, J. H. 1977 Umbilic points on Gaussian random surfaces. *J. Phys.* A **10**, 1809–1821.

Berry, M. V., Nye, J. F. & Wright, F. J. 1979 The elliptic umbilic diffraction catastrophe. *Phil. Trans. R. Soc. Lond.* A **291**, 453–484.

Callahan, J. 1977 *Geometry of* E_6 *and anorexia.* Mathematics Department, Smith College, Northampton, Mass. 01063, U.S.A. and Mathematics Institute, University of Warwick, Coventry, England. July 1977.

Nye, J. F. 1978 Optical caustics in the near field from liquid drops. *Proc. R. Soc. Lond.* A **361**, 21–41.

Pearcey, T. 1946 The structure of an electromagnetic field in the neighbourhood of a cusp of a caustic. *Phil. Mag.* **37**, 311–317.

Poston, T. & Stewart, I. 1978 *Catastrophe theory and its applications.* London: Pitman.

Tanner, L. H. 1978 A study of the optics and motion of oil droplets. *Opt. Laser Technol.* (June 1978) **10**, 125–128.

Thom, R. 1975 *Structural stability and morphogenesis: an outline of a general theory of models.* Reading, Massachusetts: W. A. Benjamin Inc.

Thorndike, A. S., Cooley, C. R. & Nye, J. F. 1978 The structure and evolution of flow fields and other vector fields. *J. Phys.* A **11**, 1455–1490.

Trinkaus, H. & Drepper, F. 1977 On the analysis of diffraction catastrophes. *J. Phys.* A **10**, L11–L16.

Whitney, H. 1955 On singularities of mappings of Euclidean spaces. I. Mappings of the plane into the plane. *Ann. Math.* **62**, 374–410.

Wright, F. J. 1977 *Wavefield singularities.* Ph.D. thesis, University of Bristol.

Zeeman, E. C. 1977 *Catastrophe theory: selected papers* (1972–1977). Reading, Massachusetts: Addison–Wesley.

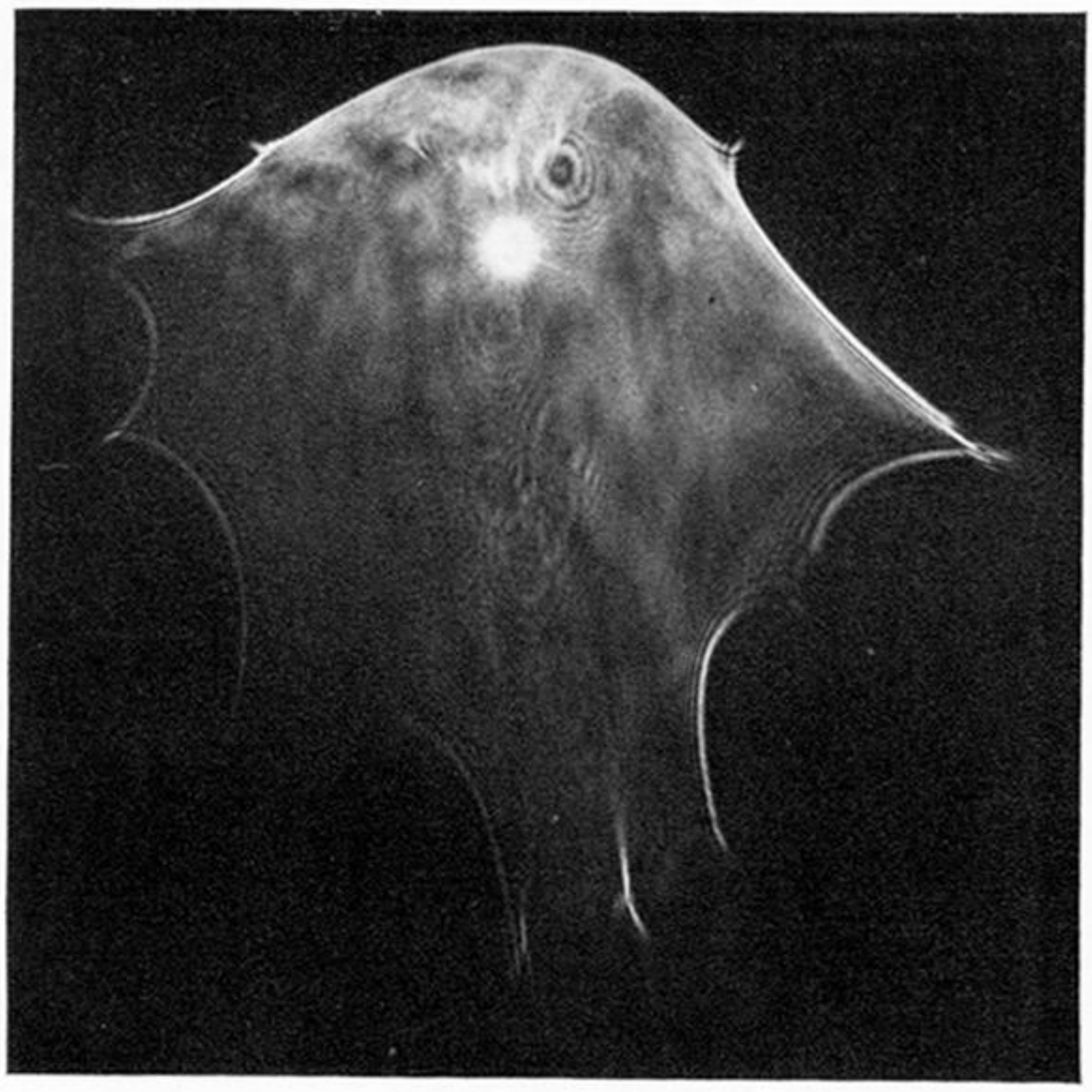

(1)

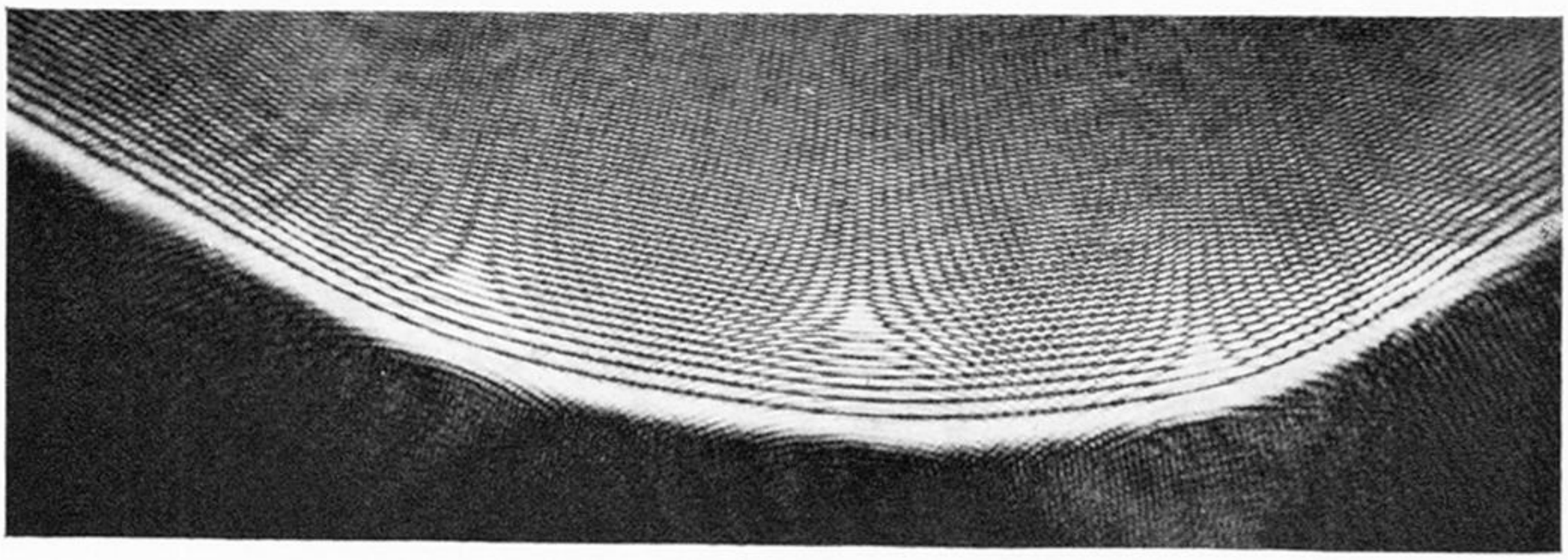

(2*a*)

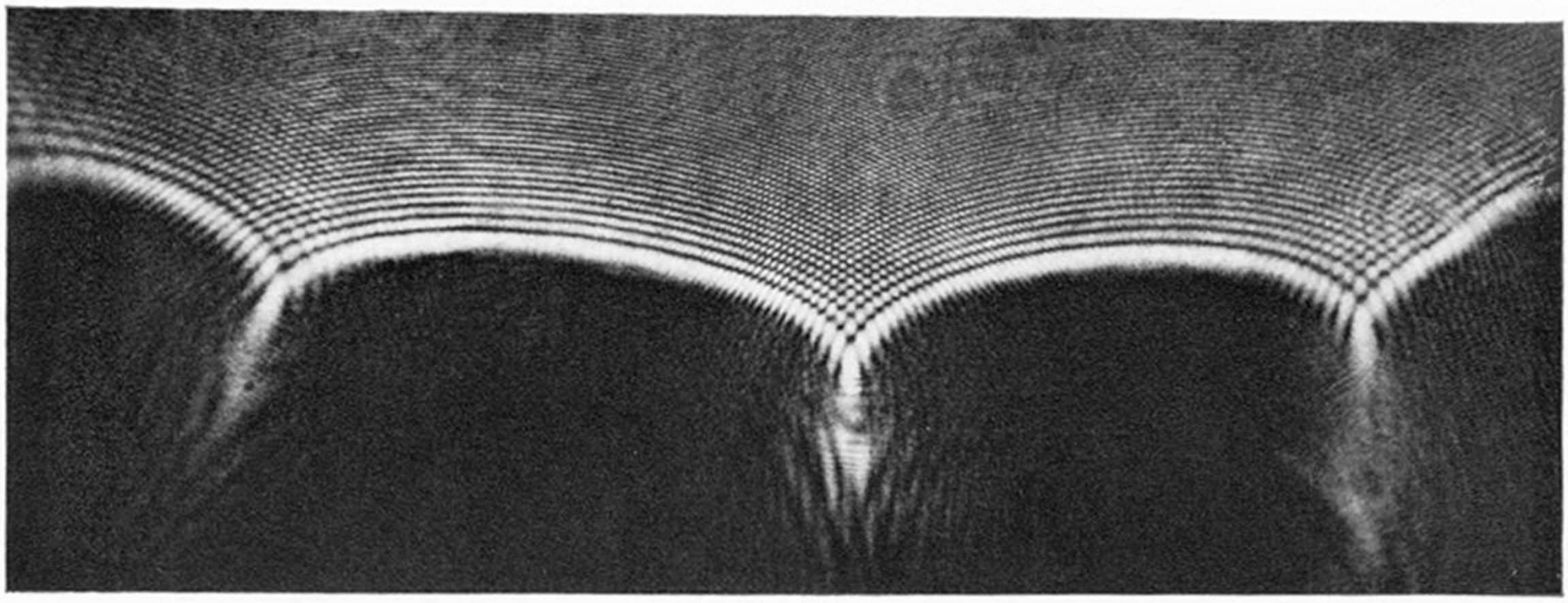

(2*b*)

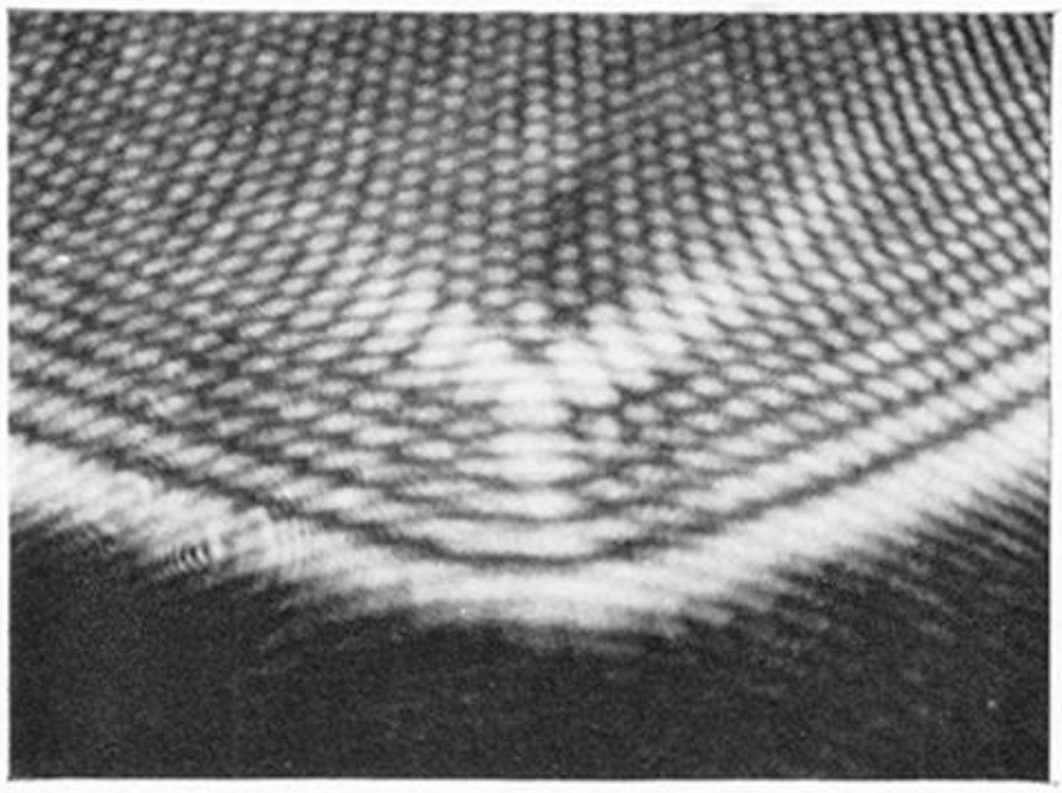

(2*c*)

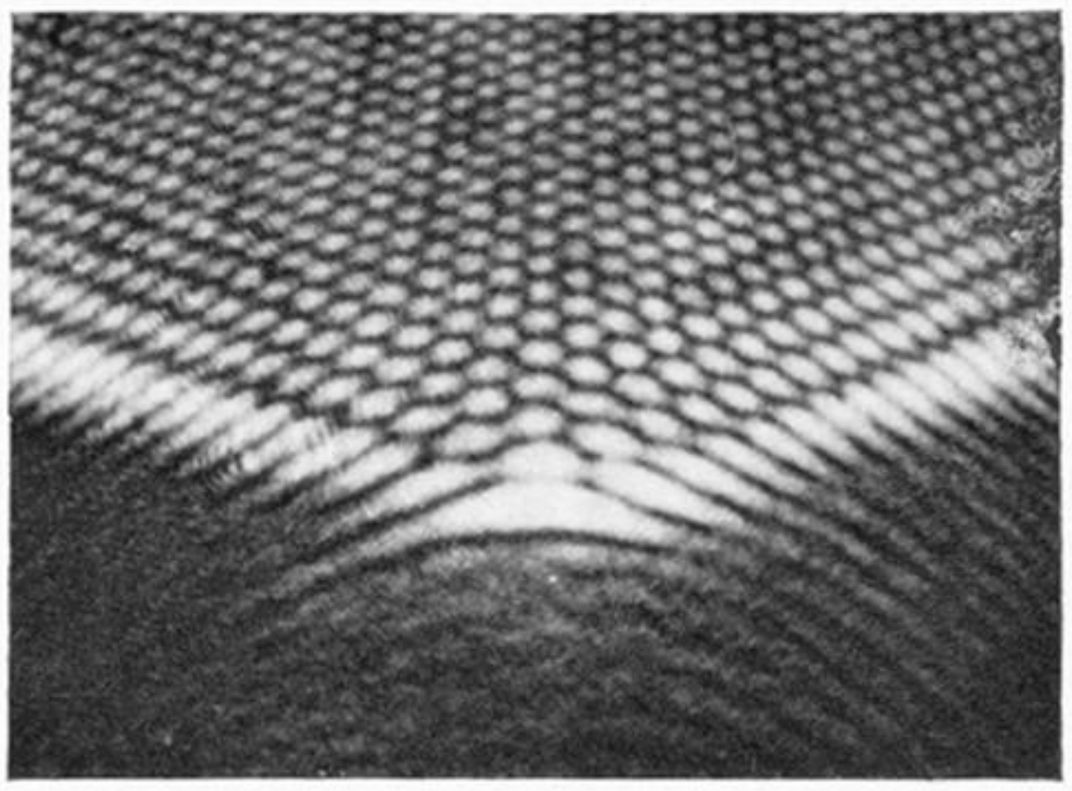

(2*d*)

FIGURES 1 AND 2. For description see opposite.

(a)

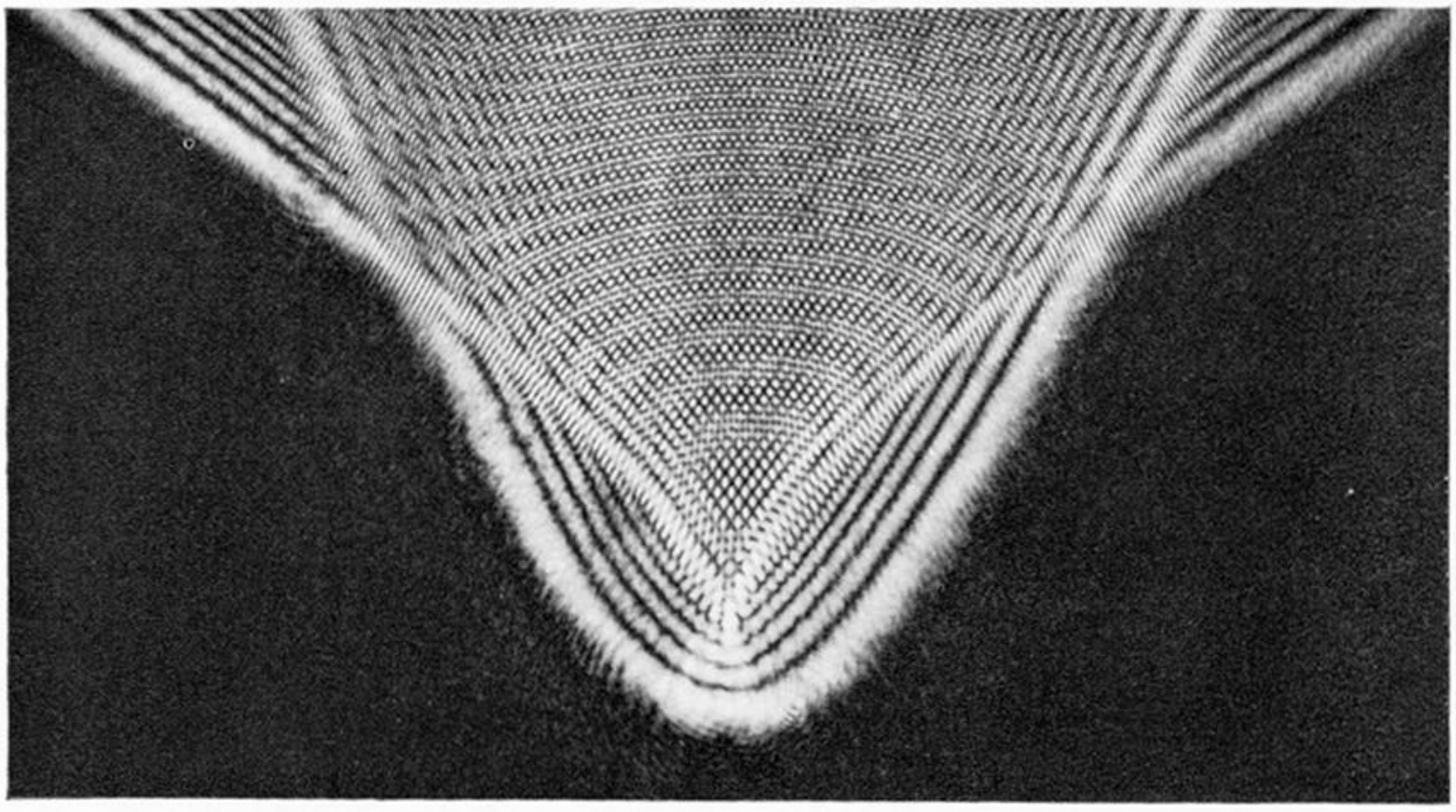

(b)

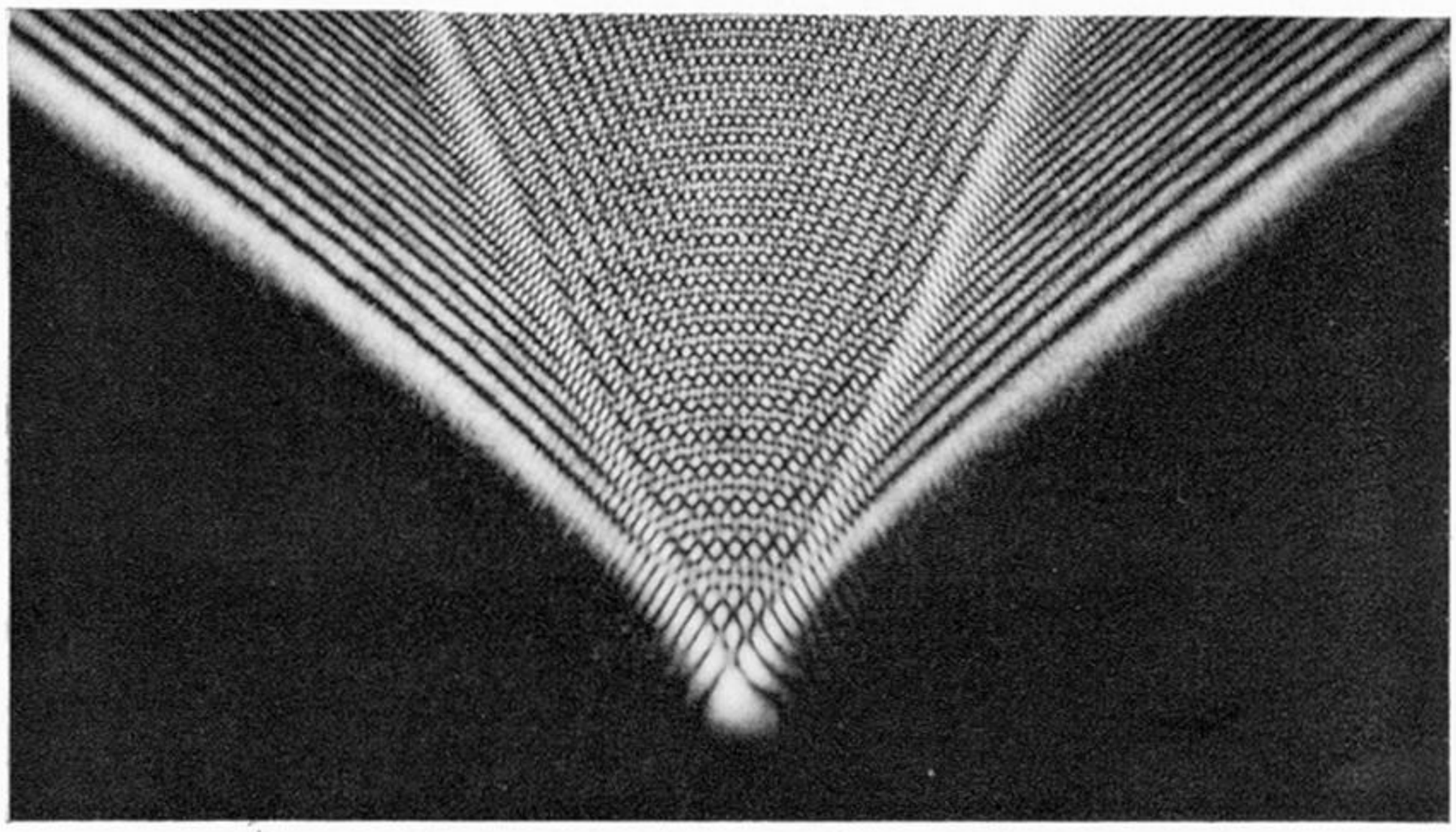

(c)

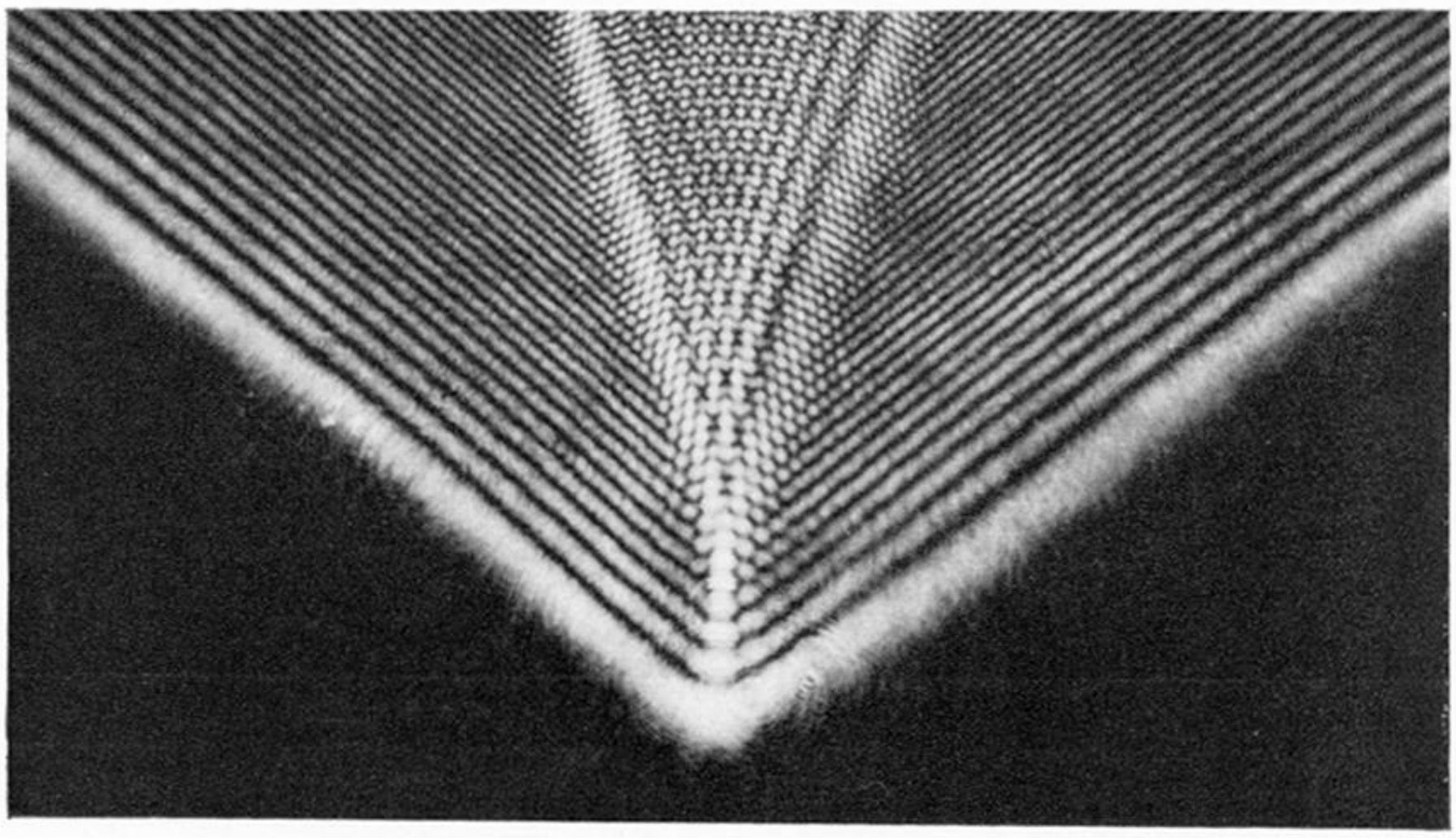

(d)

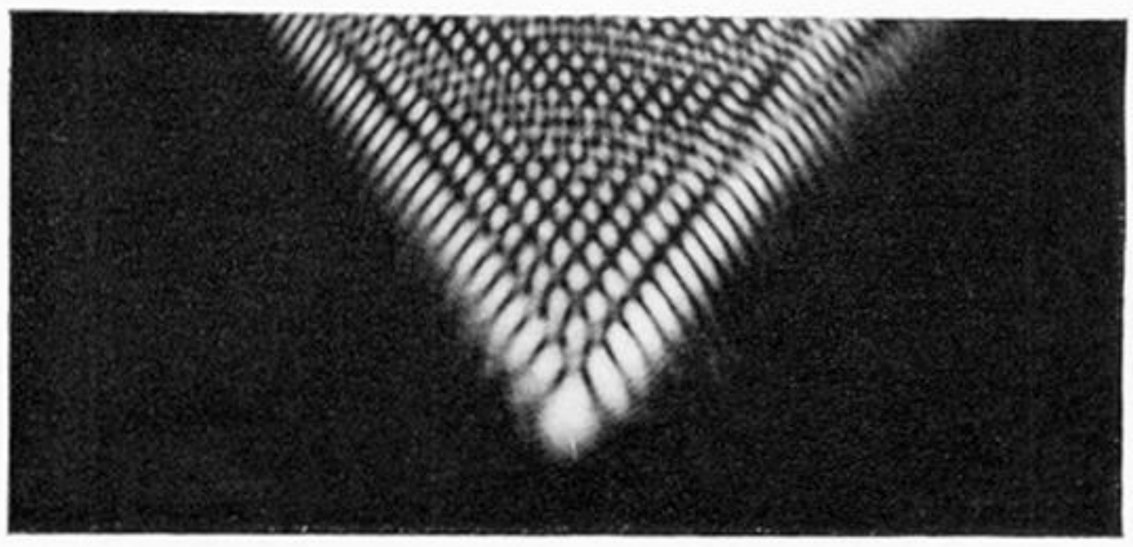

FIGURE 4. (*a*)–(*c*) Sequence through a hyperbolic umbilic focus, and (*d*) the singular section for a different drop. The edge of the drop was fixed by a circular hole, 5.5 mm in diameter, held vertically.

(a)

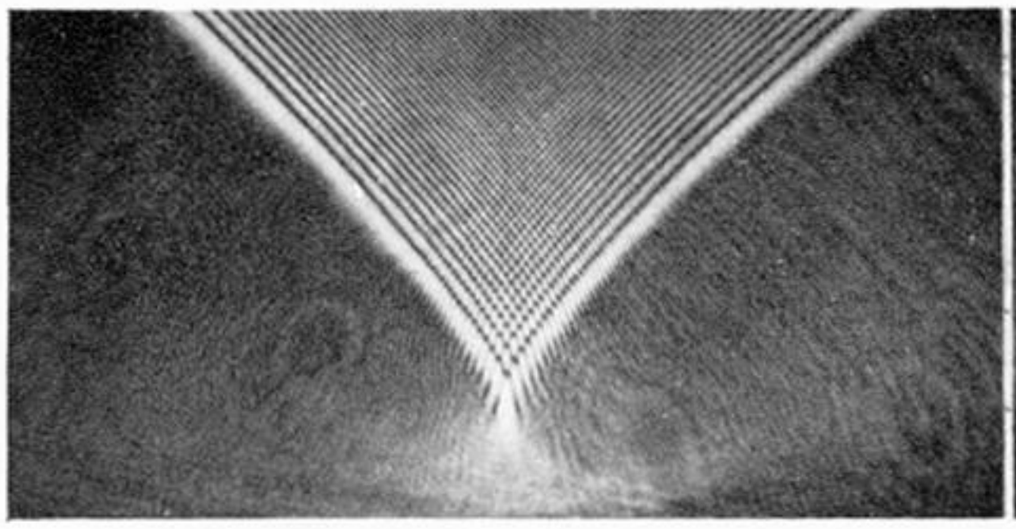

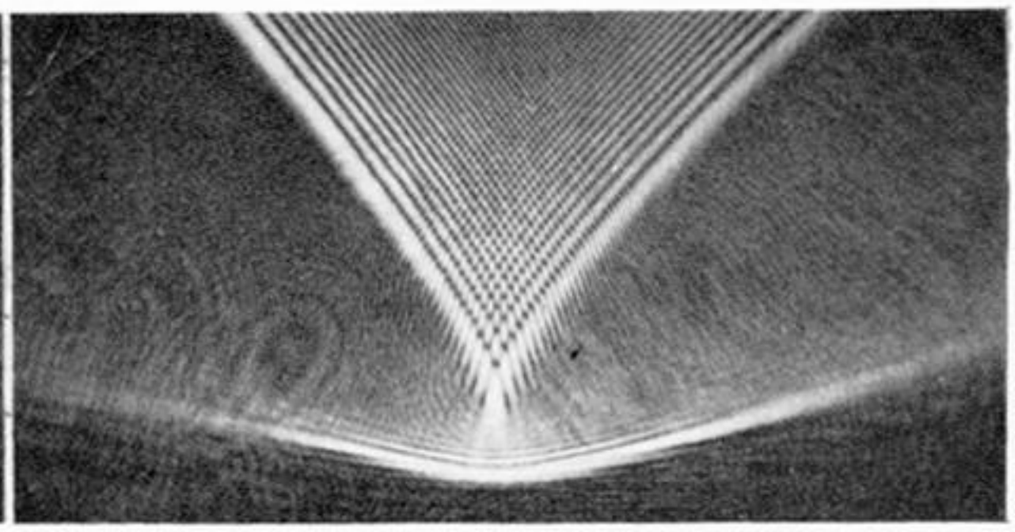

(b)

(c)

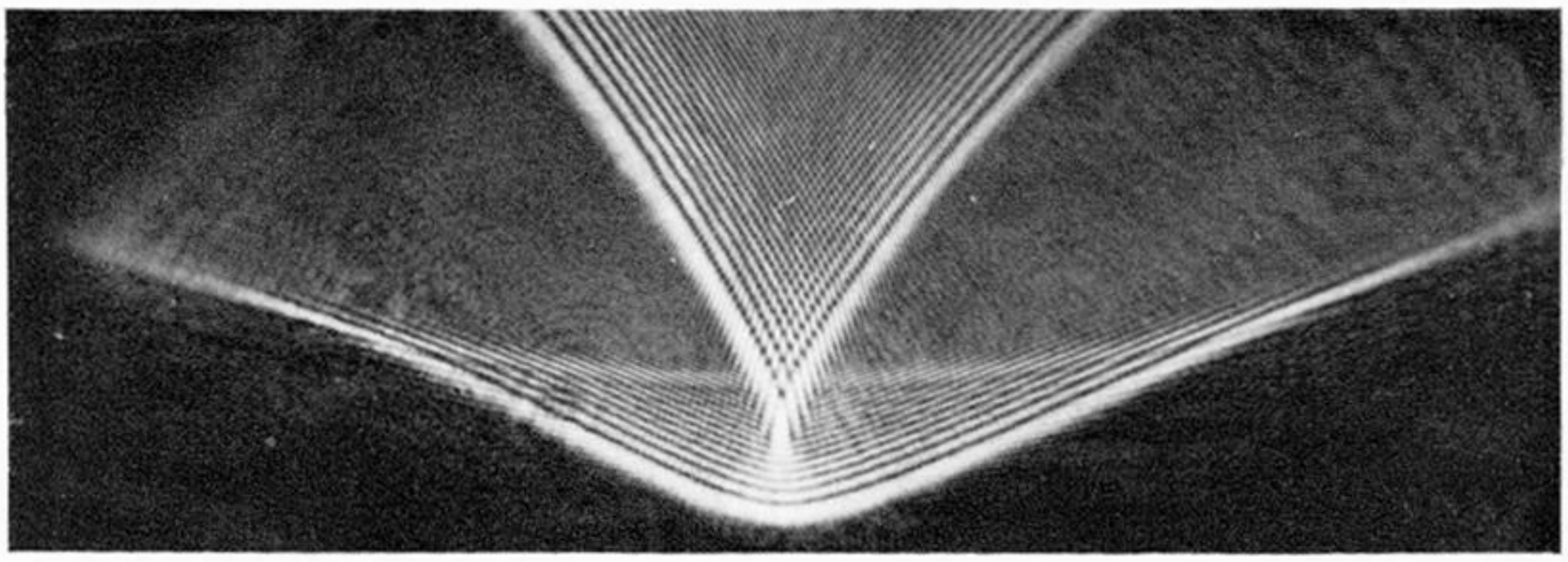

(d)

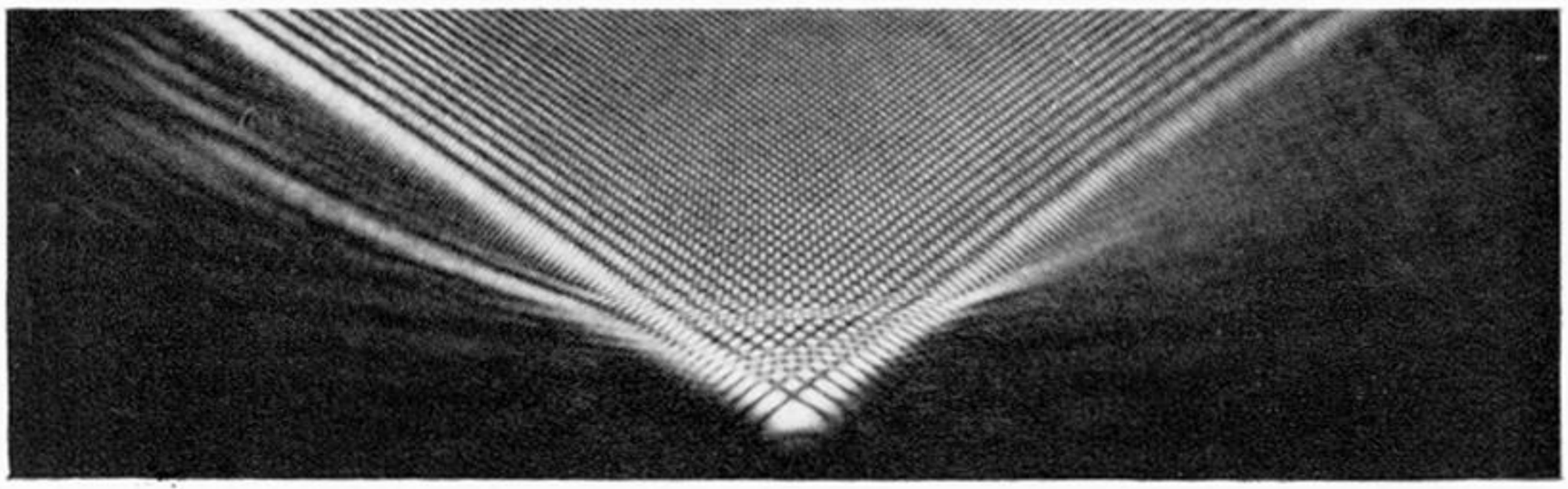

(e)

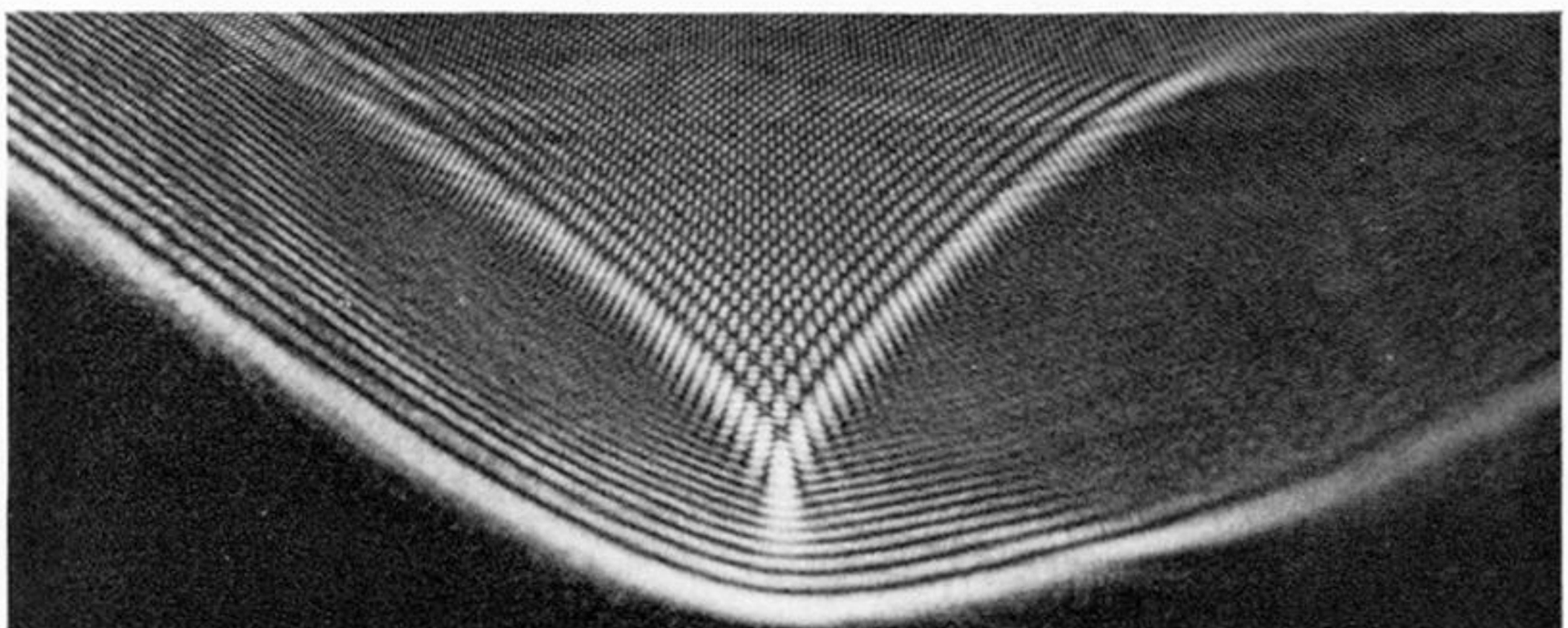

(f)

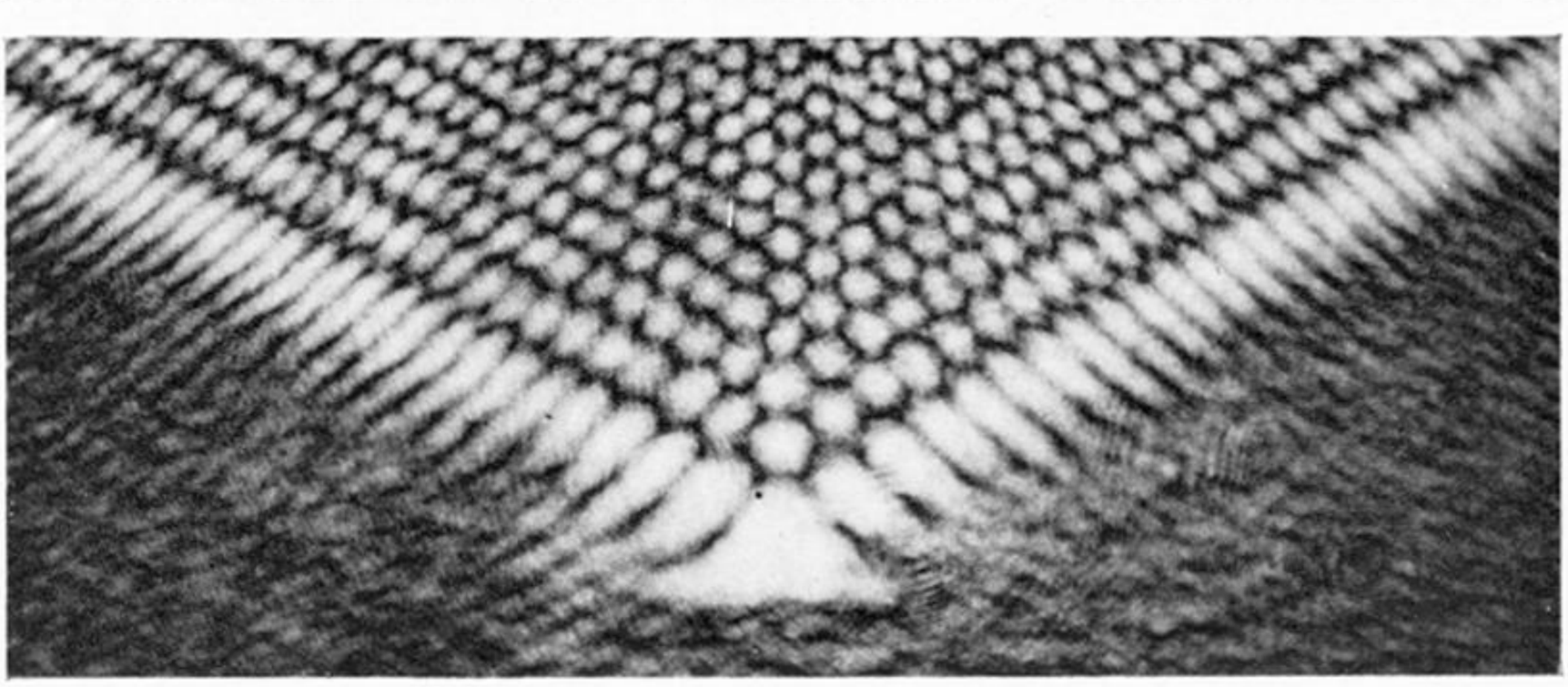

FIGURE 8. Light caustics near a parabolic umbilic focus. (*a*)–(*e*) correspond to the left hand half of figure 7. (*f*) is a section almost through the singularity itself.

(11*a*) 9, 10

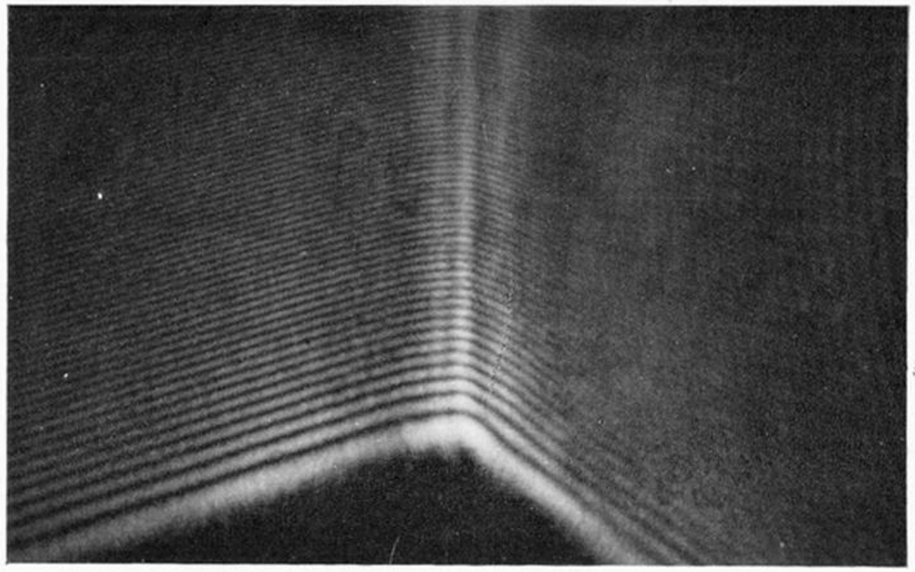

(11*b*) 5–10

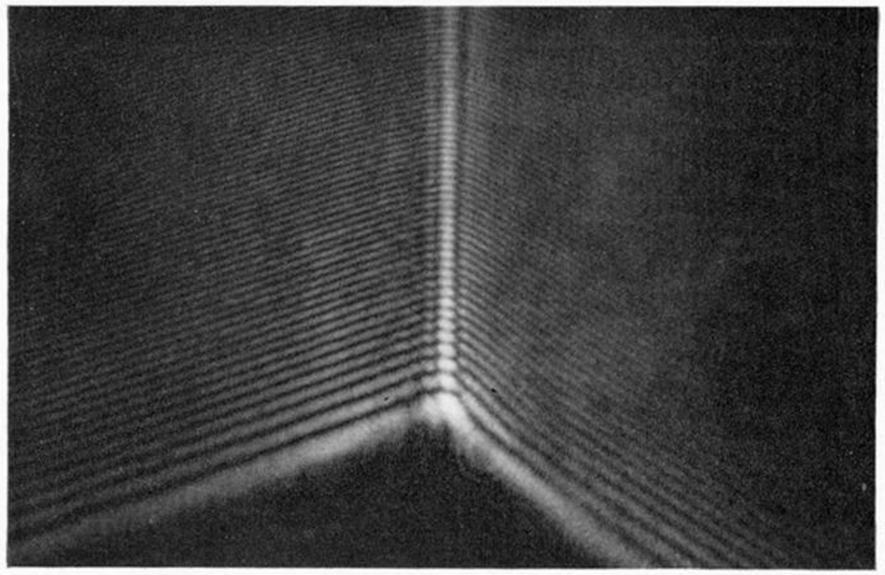

(11*c*) 5–10

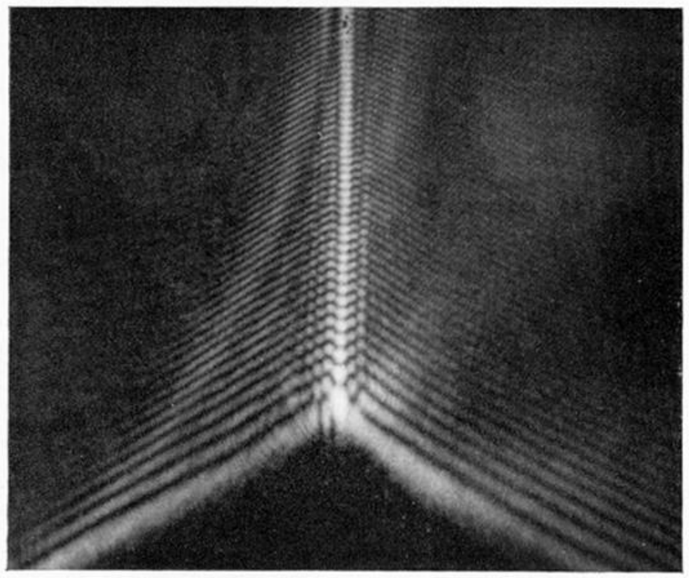

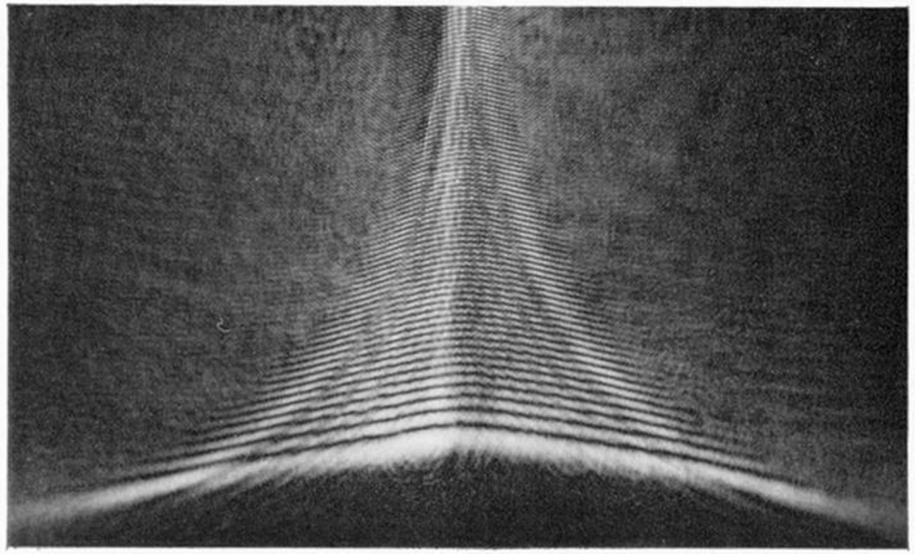

(12*a*) 11

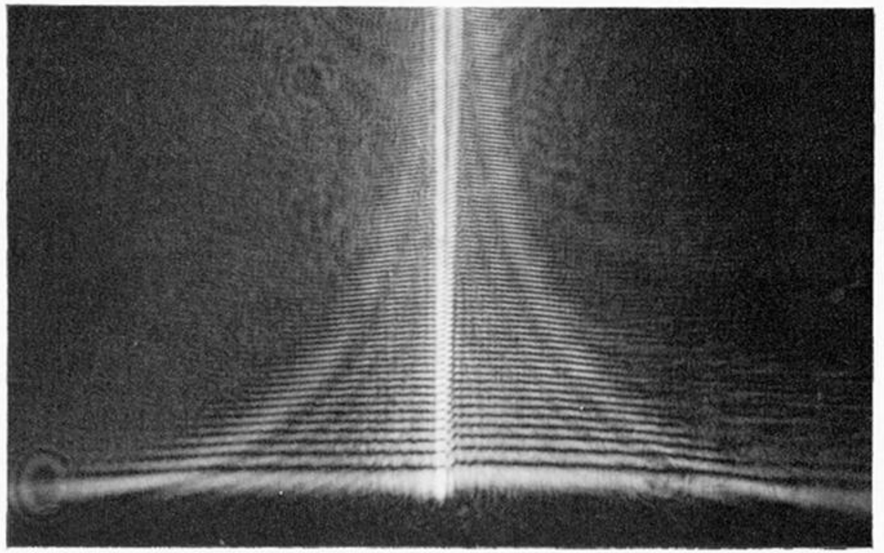

(12*b*)

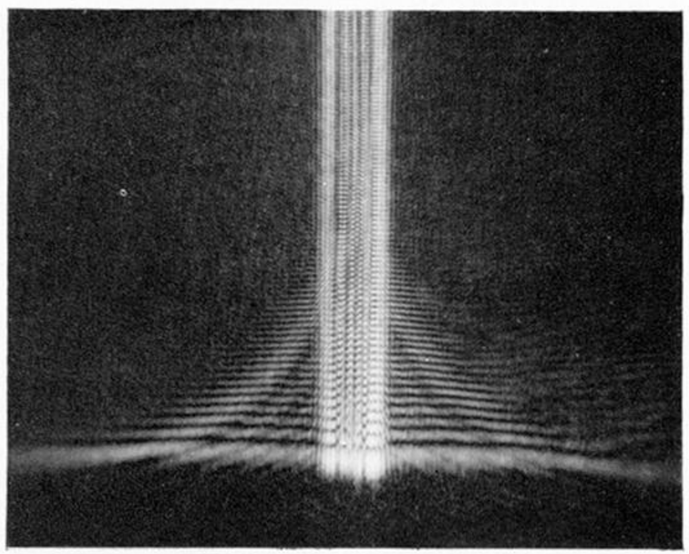

(12*c*) 1

FIGURE 11. Unfoldings of E_6 with $c = 0$, e positive and very near the origin. (*a*), (*b*) and (*c*) are all from the same drop and show the effect of moving the plane of focus of the microscope towards the drop. Substrate at 30° to horizontal. Numbers shown refer to diagrams in figure 9.

FIGURE 12. Unfoldings of E_6 with $c = e = 0$. In (*a*) to (*c*) the plane of focus of the microscope has been moved towards the drop. (*a*) d negative; (*b*) $d = 0$, singular section; (*c*) d positive.

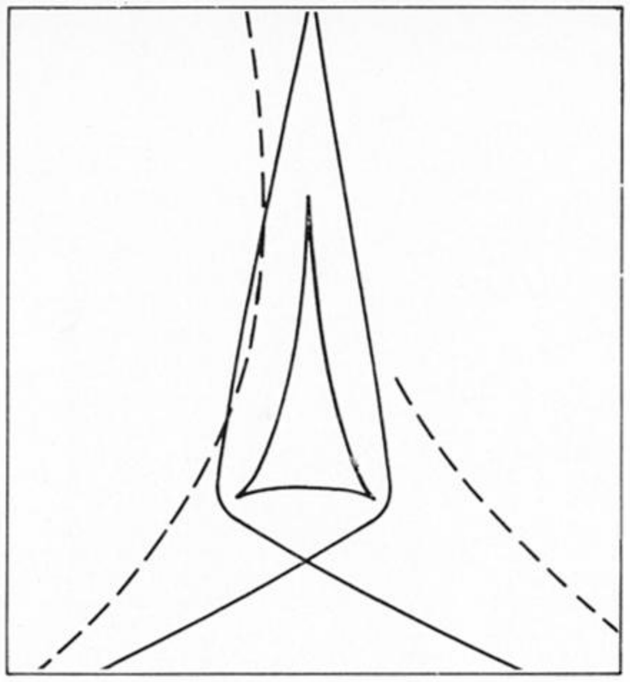

(*a*) 2

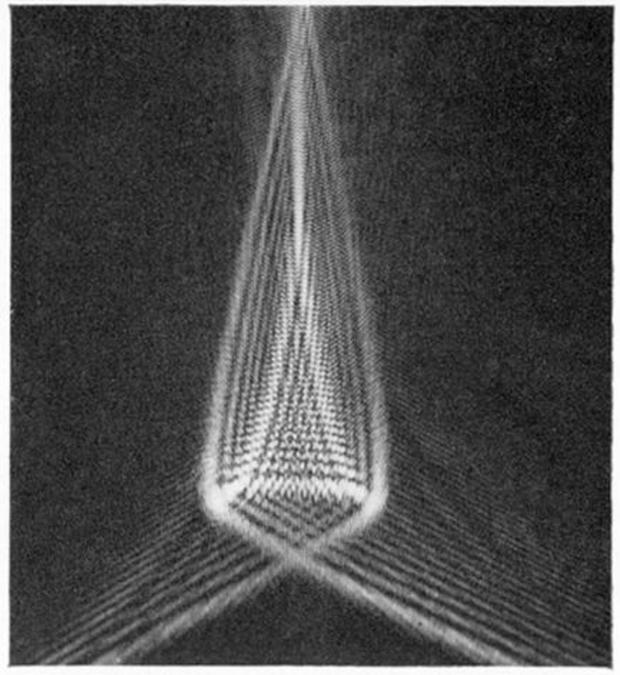

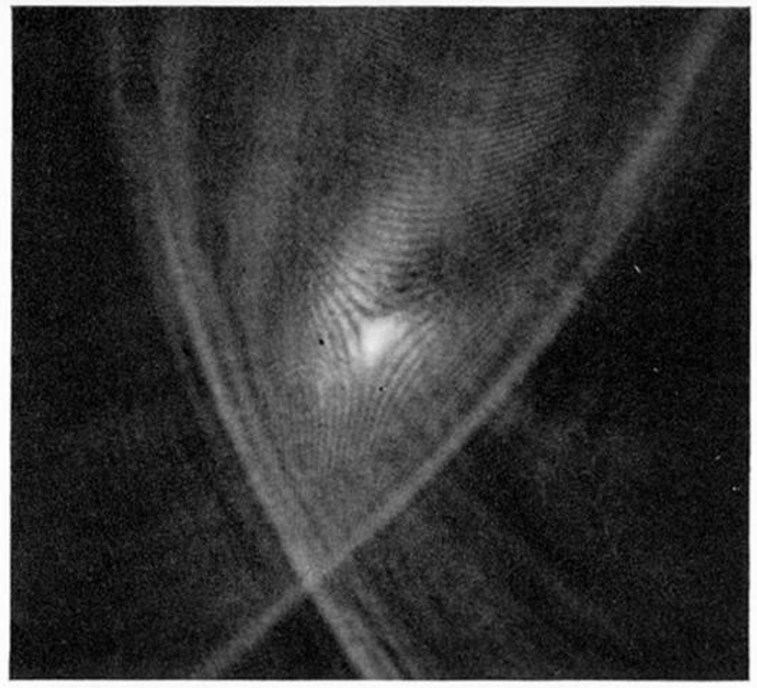

(*f*) 3

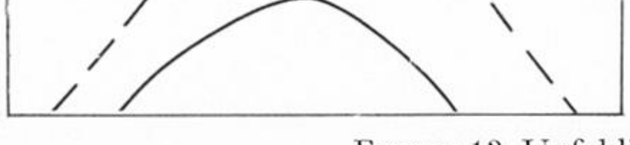

(*b*) 6

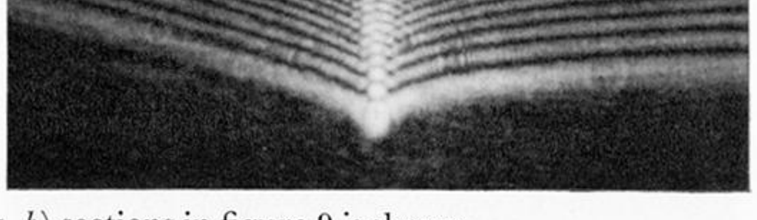

(*e*) 16

(*c*) 10

(*d*) 13

FIGURE 13. Unfoldings of E_6 with $c = 0$. The correspondence with the numbered (a, b) sections in figure 9 is shown.

(a)

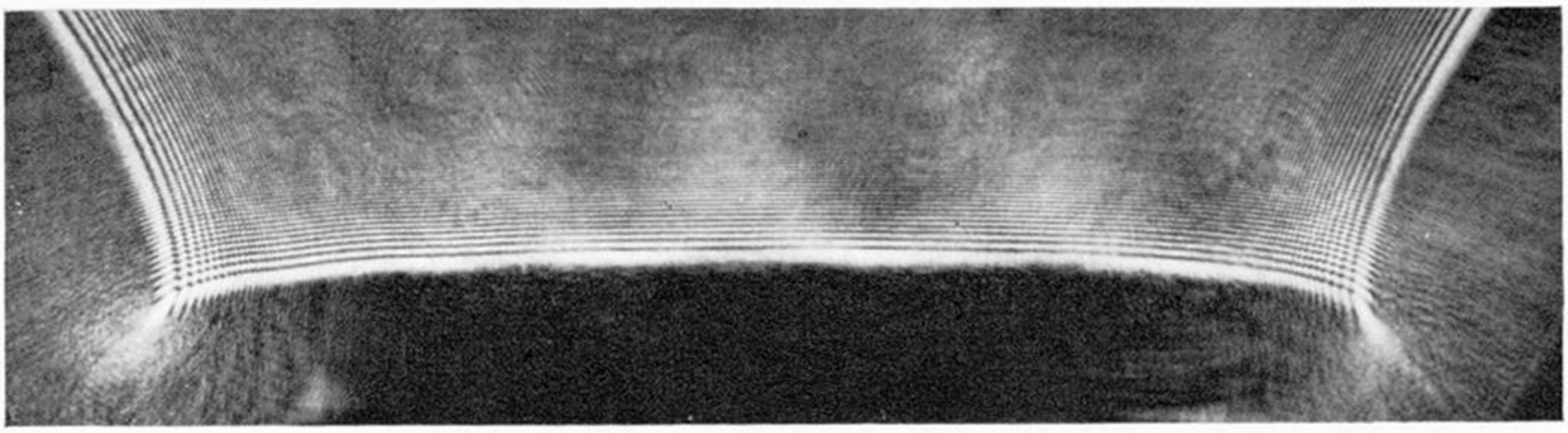

(b)

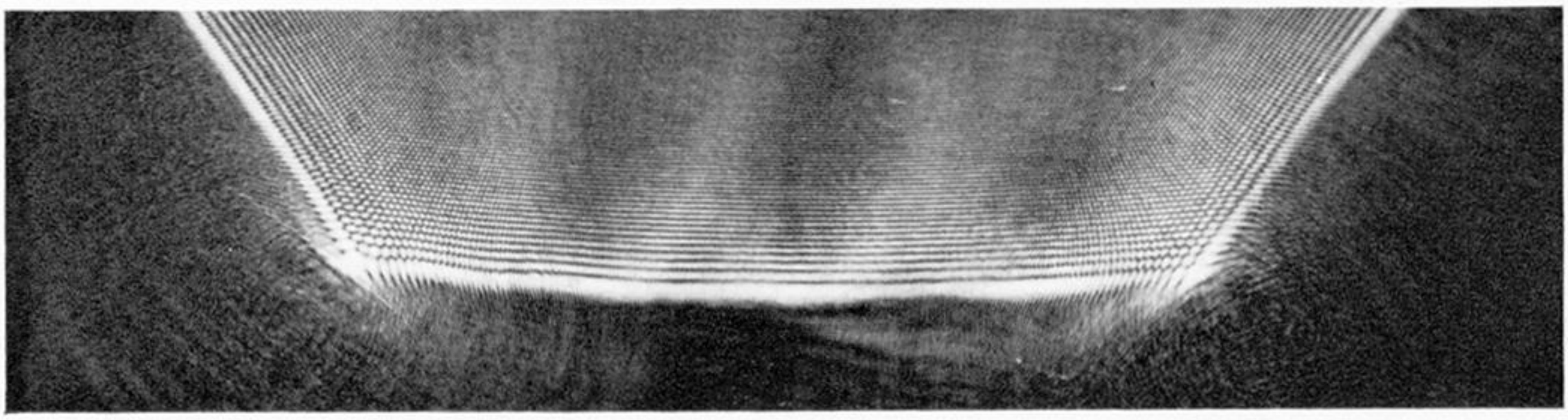

(c)

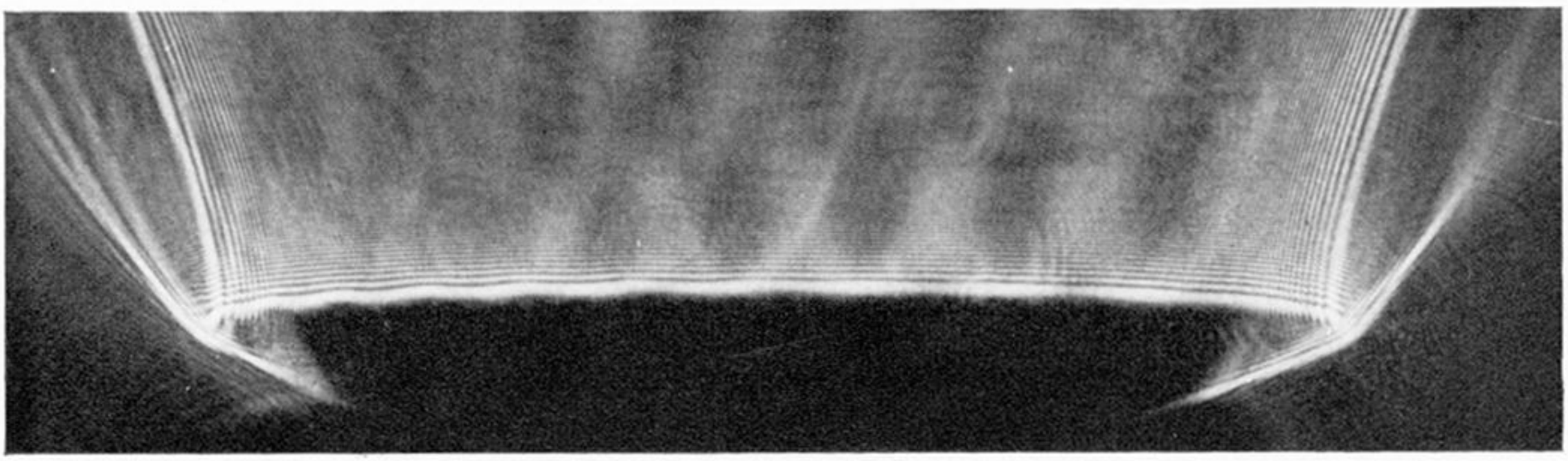

(d)

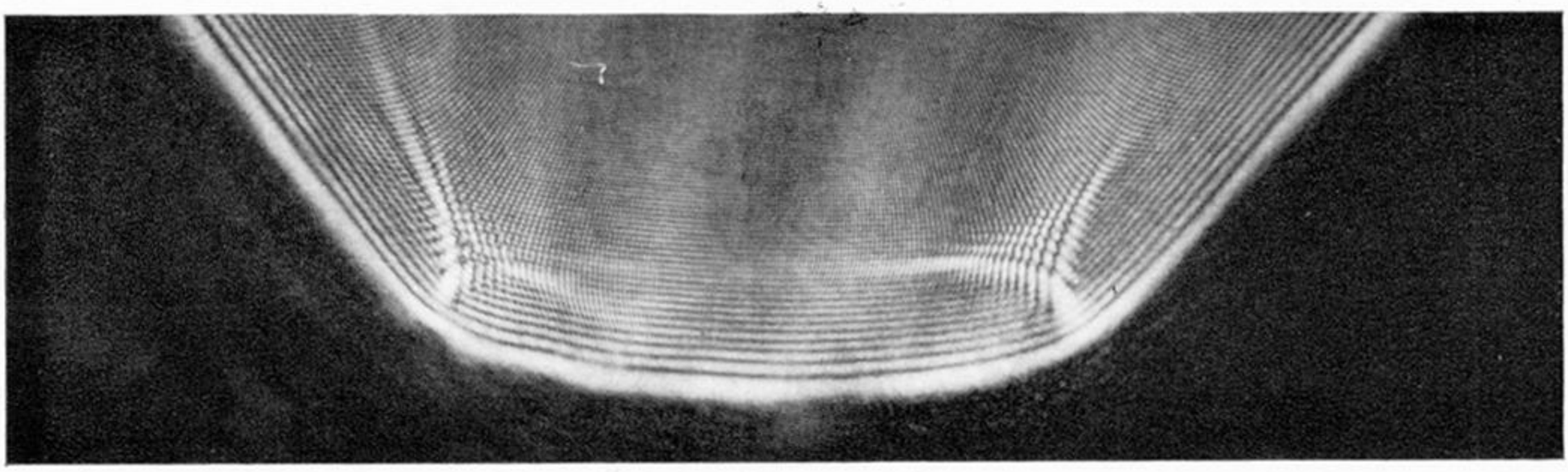

(e)

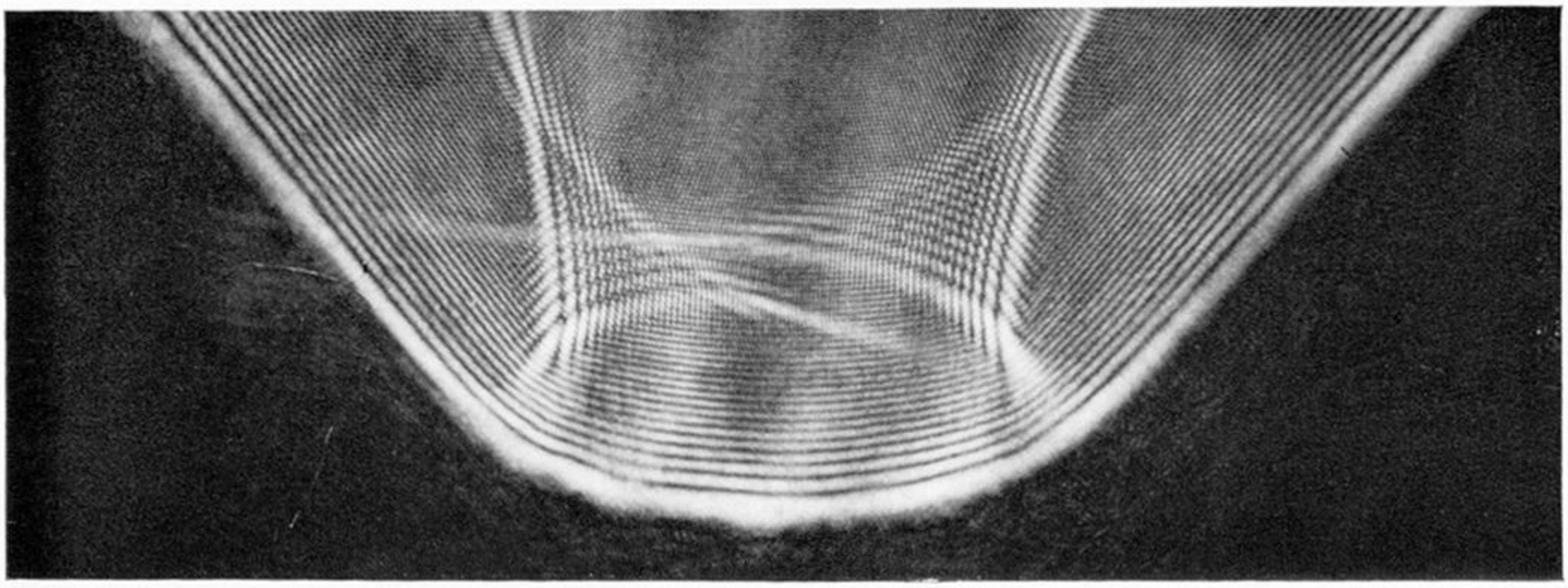

FIGURES 14(*a*)–(*e*). For description see opposite.

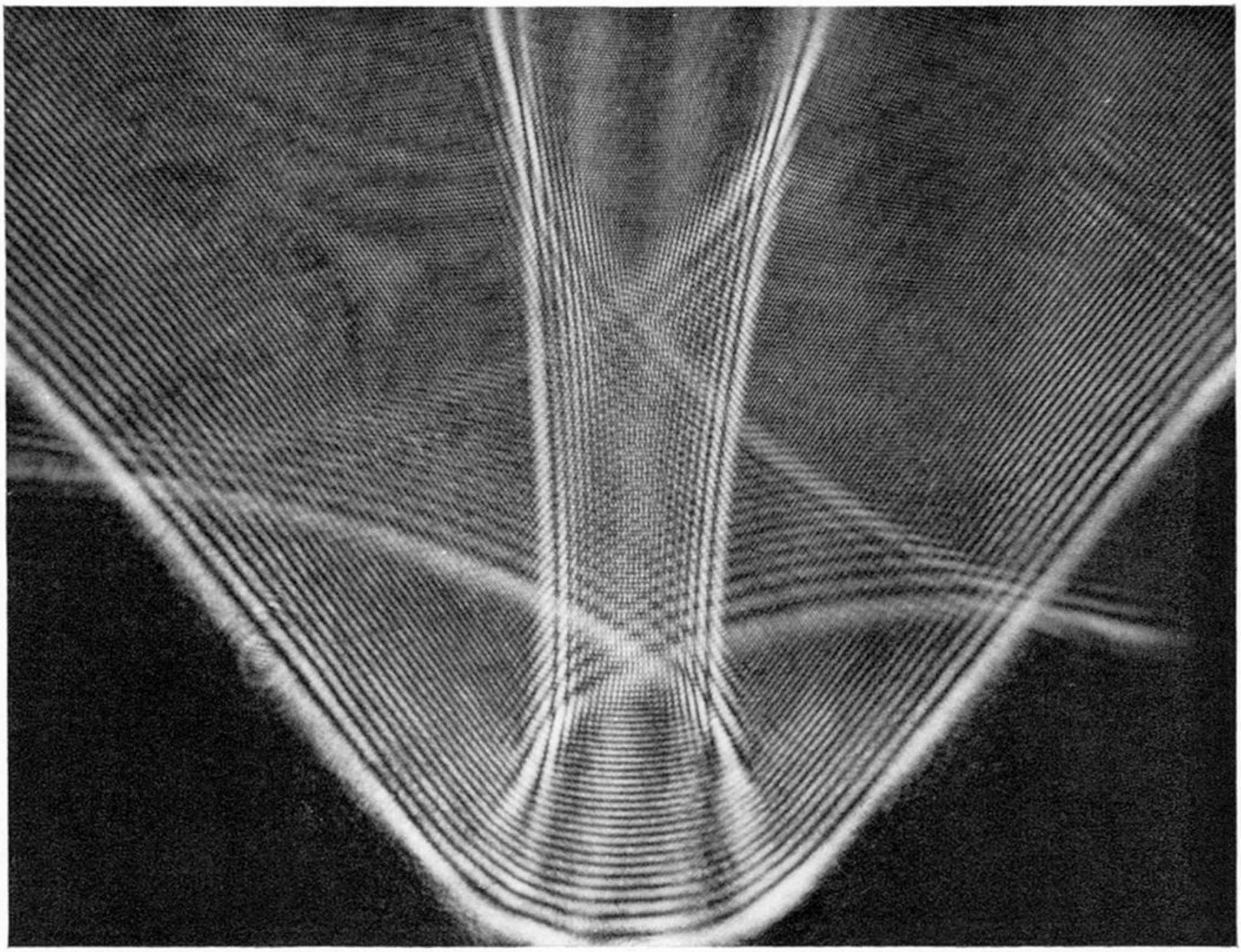

(*f*)

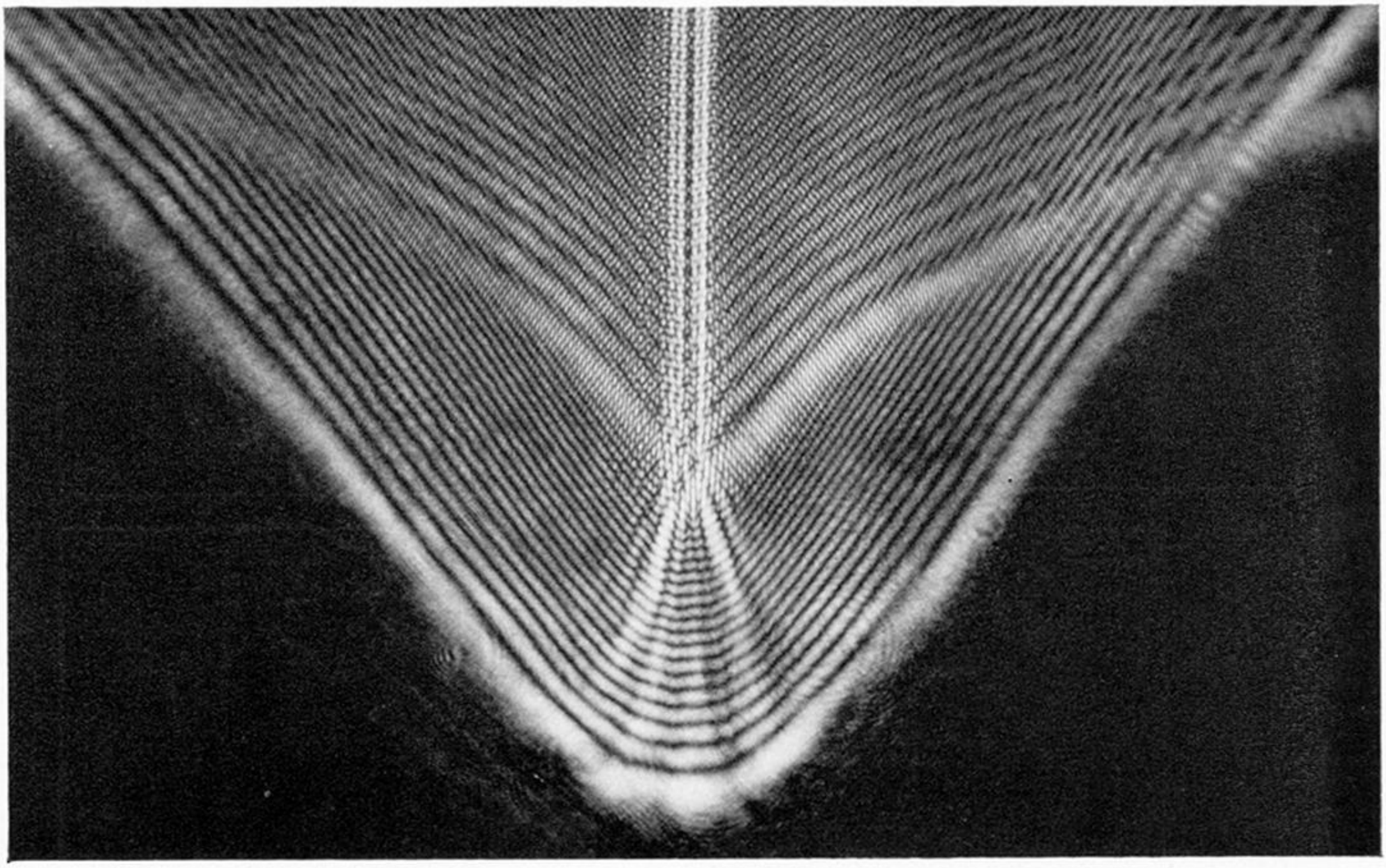

(*g*)

FIGURE 14. (*a*)–(*b*) and (*d*)–(*f*) is a focusing sequence moving away from the drop showing at (*b*) two simultaneous parabolic umbilics as part of the non-local unfolding of E_6. (*c*) is from another drop and shows lips unfolding from (*b*).

(15)

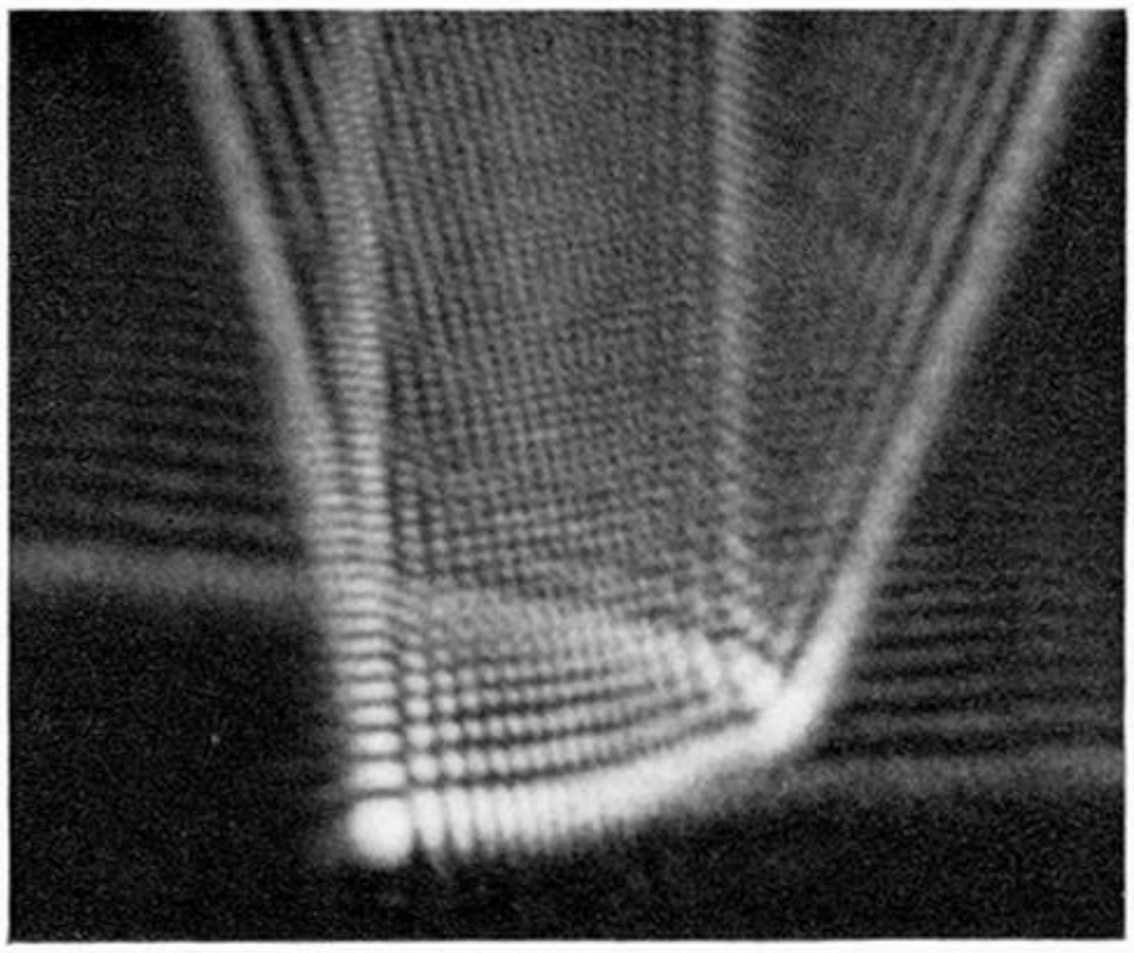

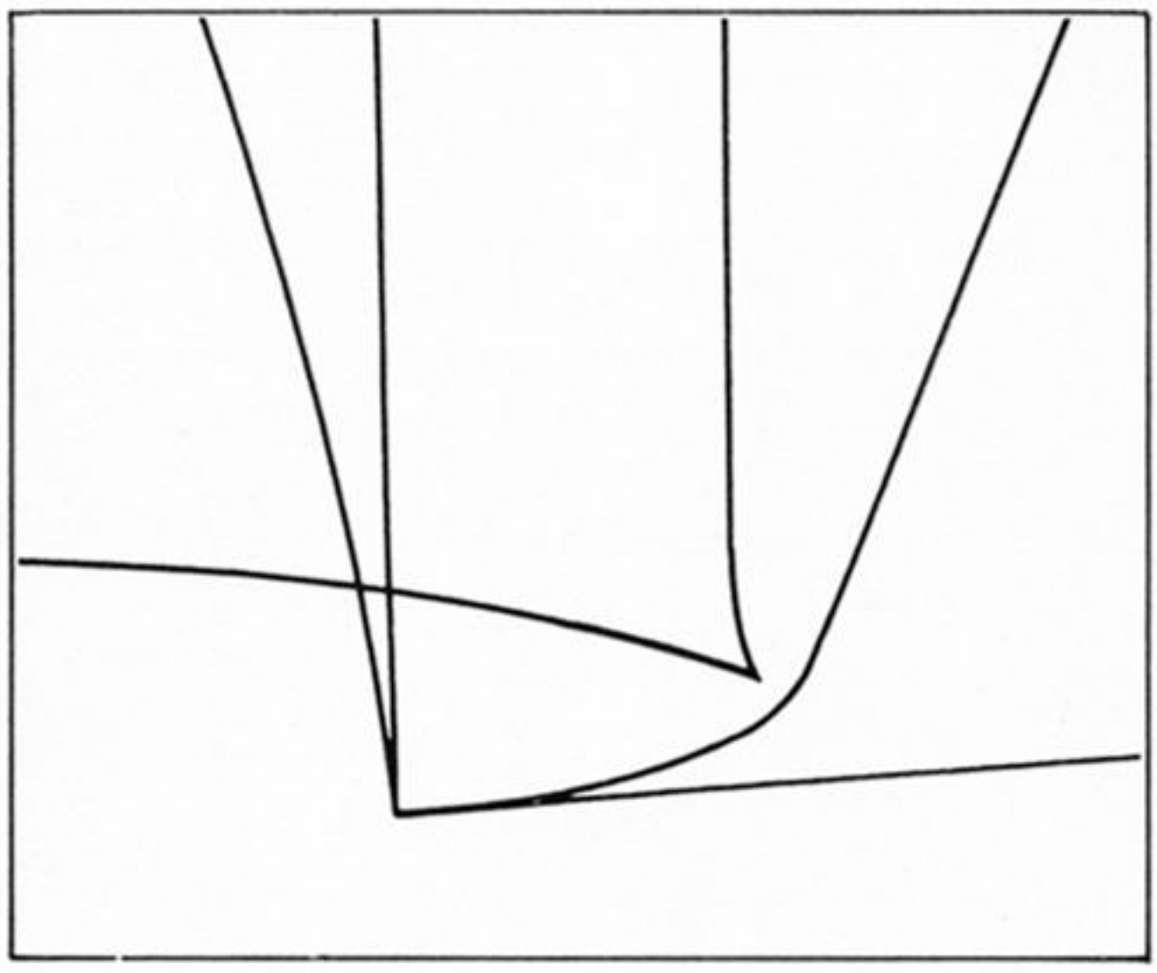

(17*a*)

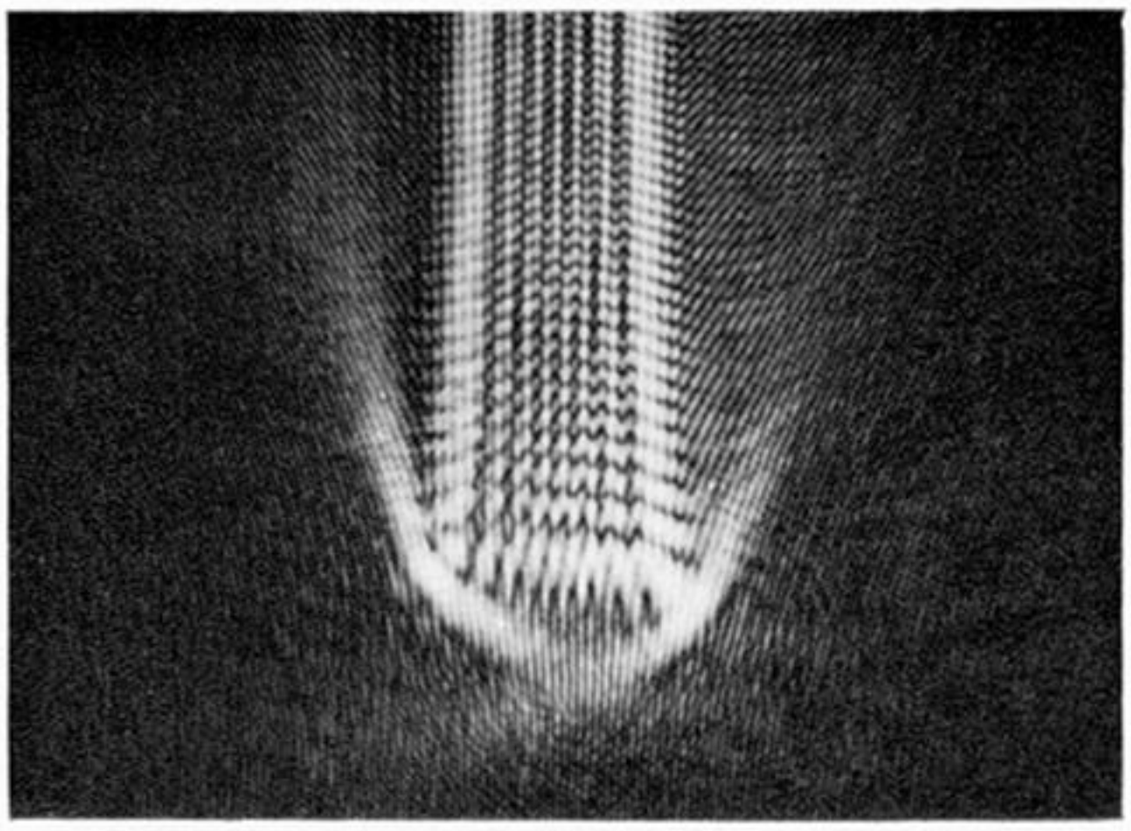

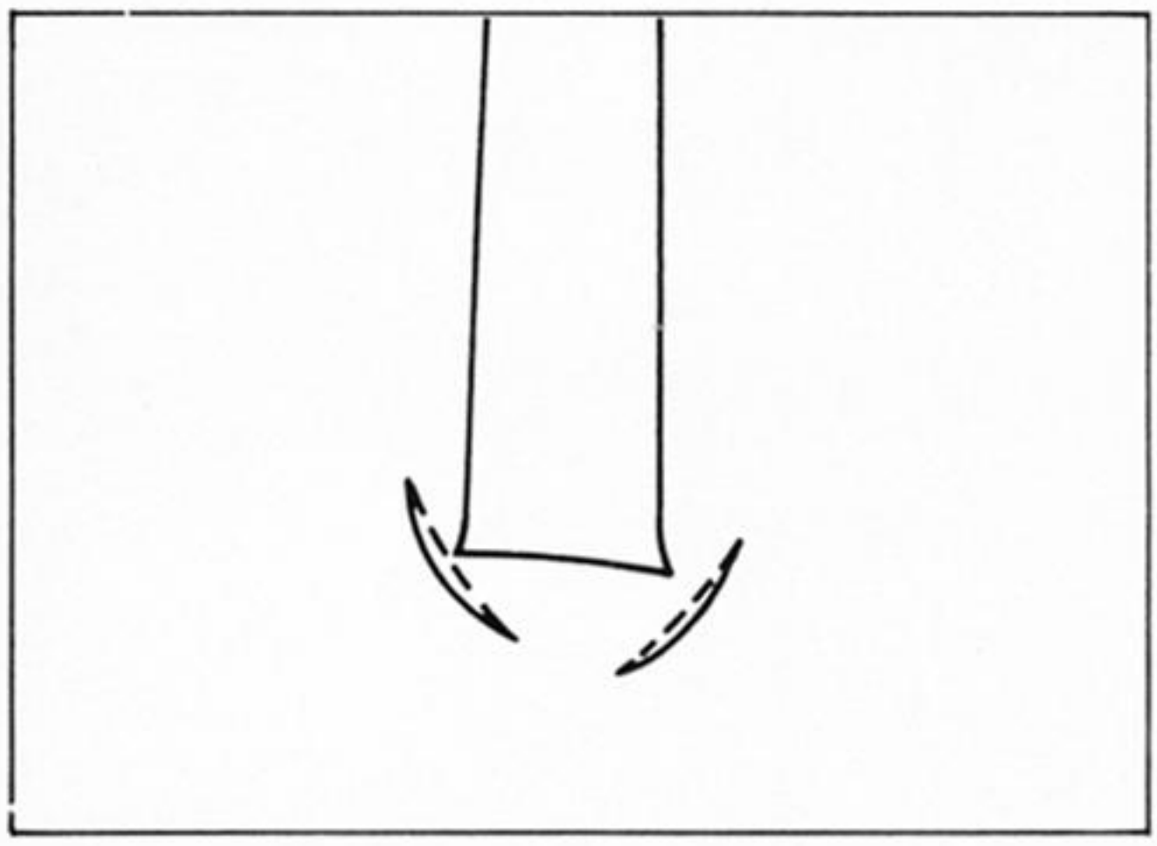

(17*b*)

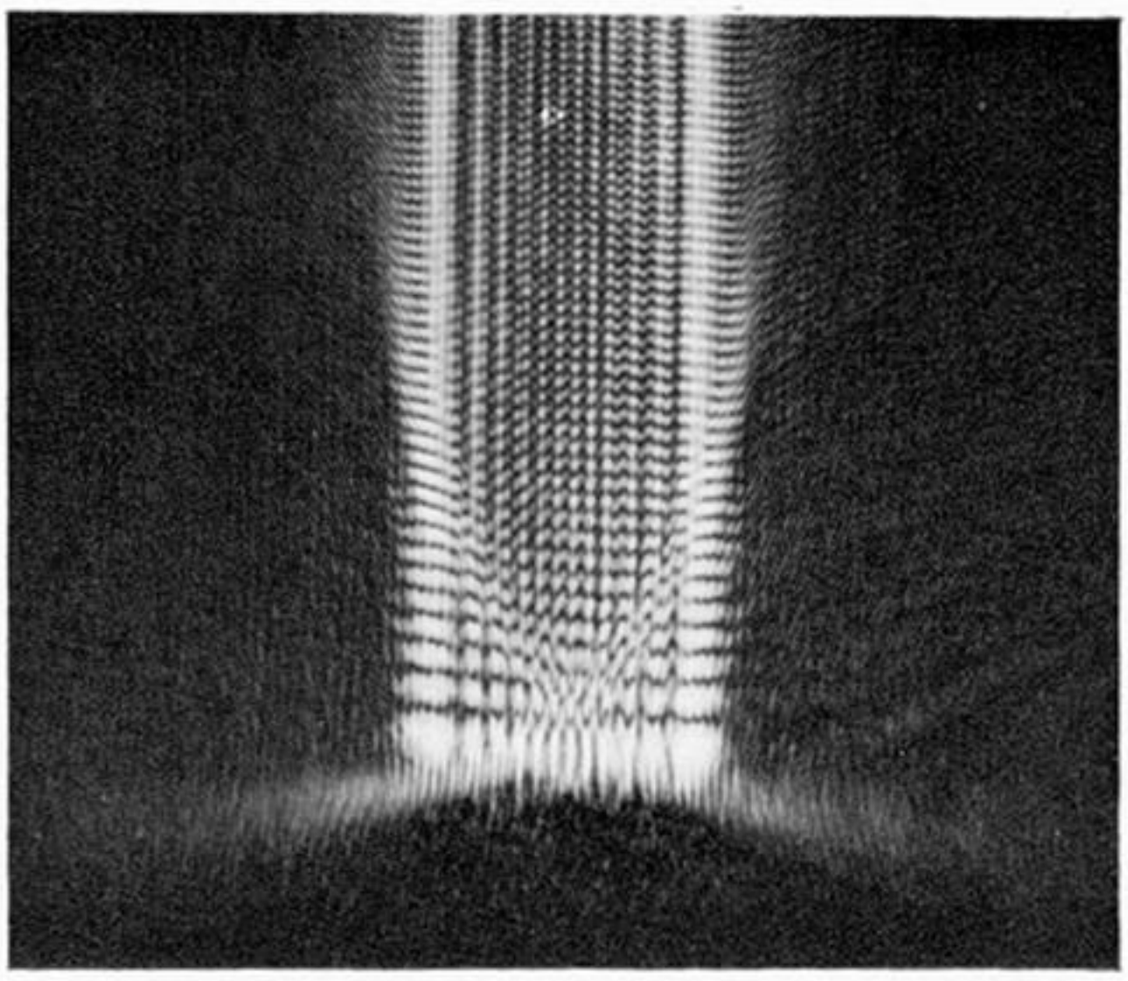

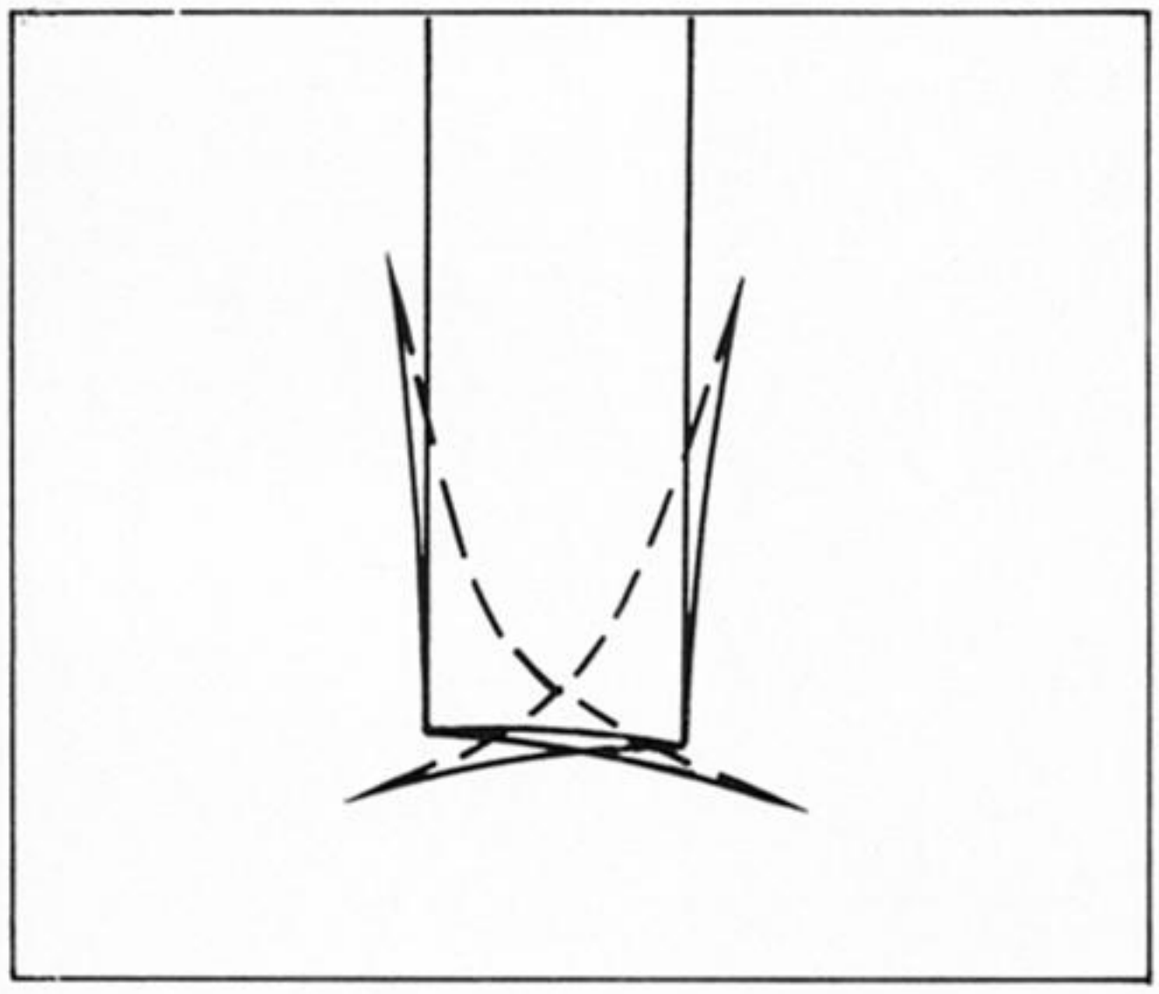

(17*c*)

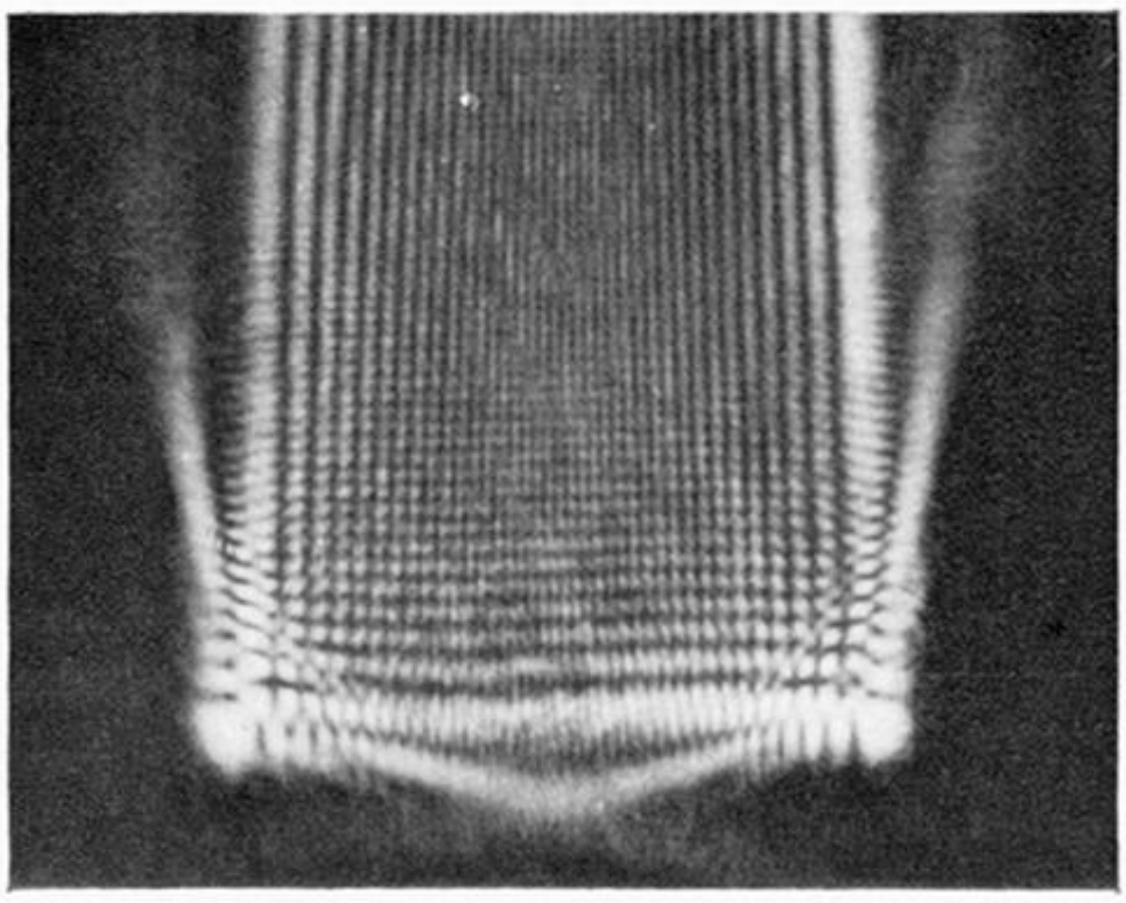

FIGURE 15. Unfolding of E_6 with $c \neq 0$.

FIGURE 17. Unfoldings of E_6 disguised by the proximity of D_5 loci.